



**USING ARGON AND HELIUM COLD PLASMA
POWER IN ETCHING THE NUCLEAR TRACK
DETECTOR CR-39**

**2024
MASTER THESIS
DEPARTMENT OF PHYSICS**

Wisam Mahmood ABBOOSH

**Thesis Advisor
Assist. Prof. Dr. Ferhat BOZDUMAN**

**USING ARGON AND HELIUM COLD PLASMA POWER IN ETCHING
THE NUCLEAR TRACK DETECTOR CR-39**

Wisam Mahmood ABBOOSH

Thesis Advisor

Assist. Prof. Dr. Ferhat BOZDUMAN

T.C.

Karabuk University

Institute of Graduate Program

Department of Physics

Master Thesis

KARABÜK

January 2024

I certify that in my opinion the thesis submitted by Wisam Mahmood ABBOOSH titled “USING ARGON AND HELIUM COLD PLASMA POWER IN ETCHING THE NUCLEAR TRACK DETECTOR CR-39” is fully adequate in scope and in quality as a thesis for the degree of Master of Science.

Assist. Prof. Dr. Ferhat BOZDUMAN
Thesis Advisor, Department of Physics

.....

This thesis is accepted by the examining committee in a unanimous vote at the Department of Physics as a Master of Science thesis. February 1, 2024

Examining Committee Members (Institutions)

Signature

Chairman : Assist. Prof. Dr. Ferhat BOZDUMAN (KBU)

.....

Member : Assist. Prof. Dr. Khalid Aal-SHABEEB (KBU)

.....

Member : Assoc. Prof. Dr. Ali GÜLEÇ (ISUBU)

.....

The degree of Master of Science by the thesis submitted is approved by the Administrative Board of the Institute of Graduate Programs, Karabük University.

Assoc. Prof. Dr. Zeynep ÖZCAN
Director of the Institute of Graduate Programs

.....

“All information in this letter has been obtained and provided by academic rules and ethical principles; I further certify that I have provided all attribution that does not arise in this work, as required by these rules and principles.”

Wisam Mahmood ABBOOSH

ABSTRACT

M. Sc. Thesis

USING ARGON AND HELIUM COLD PLASMA POWER IN ETCHING THE NUCLEAR TRACK DETECTOR CR-39

Wisam Mahmood ABBOOSH

**Karabuk University
Institute of Graduate Programs
Department of Physics**

Thesis Advisor:

Assist. Prof. Dr. Ferhat BOZDUMAN

January 2024, 51 pages

In this study, we investigated the effect of cold plasma power on the number of tracks in the nuclear track detector CR-39 when it etched. The CR-39 detectors exposed to alpha particles emitted from ^{241}Am source with activity of $1\mu\text{Ci}$ for 5min., and then etched in a cold plasma etching system. The plasma power was 7W, Voltage: 10kV, Frequency: 10kHz, Gas Flow Rate: 4lt/min, Working Distance: 1-2cm, Parameters given above are the same for both gases (Argon and Helium). The number of tracks analyzed using an optical microscope. Our results showed that the plasma power significantly affected the number of tracks for both gases. The number of tracks increased with increasing plasma power. We also found that the optimal conditions for Argon gas obtaining a high track density ($3944.773\text{ tracks/mm}^2$) at time 40 min for a distance 3mm. Optimal conditions for Helium gas obtaining a high track density ($6081.525\text{ tracks/mm}^2$) at time 40 min. for a distance 3mm. The results show that the track density increases with increasing exposure time to the plasma

until we get the maximum then decreases, and track density increases with decreasing the distance between plasma and the detector. Results are important for optimizing the cold plasma etching process of CR-39 detectors for various nuclear applications.

Keywords : Cold plasma, gas flow rate, track density, track radius, nuclear track detector, CR39.

Science Code : 20219

ÖZET

Yüksek Lisans Tezi

CR-39 NÜKLEER IZ DEDEKTÖRÜNÜN AŞINDIRILMASINDA ARGON VE HELYUM SOĞUK PLAZMA GÜCÜNÜN KULLANILMASI

Wisam Mahmood ABBOOSH

Karabük Üniversitesi

Lisansüstü Eğitim Enstitüsü

Fizik Anabilim Dalı

Tez Danışmanı:

Dr. Öğr. Üye. Ferhat BOZDUMAN

Ocak, 2024, 51 Sayfa

Bu çalışmada, soğuk plazma gücünün CR-39 nükleer iz detektörü aşındırıldığında iz sayısı üzerindeki etkisini araştırdık. CR-39 dedektörleri, 5dakika boyunca 1µci aktiviteyle 241Am kaynağından yayılan alfa parçacıklarına maruz bırakıldı ve daha sonra soğuk bir plazma aşındırma sisteminde kazındı.

Plazma çalışma parametreleri olarak gücü 7W, Voltaj: 10kV, Frekans: 10kHz, Gaz Akış Hızı:4lt/dk, Çalışma Mesafesi:1-2cm değerlerine sabitlendi. Yukarıda verilen parametreler her iki gaz (Argon ve Helyum) için aynıdır. Optik mikroskop kullanılarak iz sayısı analiz edildi. Sonuçlarımızda plazma gücünün her iki gaz için de iz sayısını önemli ölçüde etkilediğini gösterdi. Plazma gücünün artmasıyla birlikte iz sayısı da arttı. Ayrıca Argon gazı için en uygun koşulların 3 mm'lik bir mesafe için 40 dakikada yüksek bir iz yoğunluğu (3944.773 iz/mm²) elde ettiğini bulduk. 40 dakikada yüksek bir iz yoğunluğu (6081.525 iz/mm²) elde eden Argon gazı için en

uygun koşulun 3 mm'lik çalışma mesafesi için olduğuna karar verdik. Sonuçlar, maksimuma ulaşana kadar plazmaya maruz kalma süresinin artmasıyla iz yoğunluğunun arttığını, ardından azaldığını ve plazma ile dedektör arasındaki mesafenin azalmasıyla iz yoğunluğunun arttığını göstermektedir. Sonuçlar, çeşitli nükleer uygulamalar için CR-39 dedektörlerinin soğuk plazma aşındırma işleminin optimize edilmesi açısından önemlidir.

Anahtar Kelimeler : Soğuk plazma, gaz akış hızı, iz yoğunluğu, iz yarıçapı, nükleer iz dedektörü, CR-39.

Bilim Kodu : 20219

ACKNOWLEDGMENTS

At first, I thank God who is the first, last and only helper who gives me the greatest blessing for guiding me to the correct way and the most important reason that led me to this success.

Assist Prof. Dr. Ferhat BOZDUMAN, I would like to express my deep gratitude for his invaluable support, assistance, advice and supervision. I extend my sincere thanks to Assist Prof. Dr. Khalid Aal-SHABEEB who helped me with all the details, and I thank him for his cooperation with me, and his good treatment. I also extend my sincere thanks to my teachers and I thank them. Karabük University for the facilities provided to me.

I also extend my thanks to my friends and everyone who was with me on this journey.

To my father, mother and siblings, thank you for everything you have done for me.

("This work was supported by the Research Fund of the Karabük University Project)

CONTENTS

	<u>Page</u>
APPROVAL.....	ii
ABSTRACT.....	iv
ÖZET.....	vi
ACKNOWLEDGMENTS	viii
CONTENTS.....	ix
LIST OF FIGURES	xi
LIST OF TABLES	xiii
SYMBOLS AND ABBREVIATIONS INDEX.....	xiv
PART 1	1
INTRODUCTION	1
1.1. PROBLEM STATEMENT	3
1.2. RESEARCH OBJECTIVES.....	4
1.3. STUDY QUESTIONS	4
1.4. SIGNIFICANCE OF THE STUDY	5
PART 2	6
LITERATURE REVIEW.....	6
2.1. STUDY HYPOTHESIS	11
PART 3	12
THEORETICAL BACKGROUND.....	12
3.1. DETECTION PRINCIPLE	12
3.2. REAGENT TYPES:	15
3.2.1. Inorganic Detectors.....	15
3.2.2. Organic Detectors	15
3.3. POLYMER NUCLEAR TRACK DETECTOR CR-39.....	16
3.4. SOME SKIM EFFECT COEFFICIENTS.....	17
3.4.1. Rate of Bulk Etch (V_B)	17

	<u>Page</u>
3.4.2. Track Etch Rate V_T	17
3.4.3. Etching Rate Ratio V	17
3.4.4. The Critical Angle θ_c	18
3.4.5. Efficiency of the Detector to Record the track) η).....	18
3.5. COLD PLASMA.....	18
3.6. COLD PLASMA IS CREATED.....	19
3.7. GAS HELIUM.....	19
3.8. USING COLD PLASMA TO SANITISE SURFACES.....	20
3.9. DRY ETCHING.....	21
PART 4.....	22
METHODOLOGY.....	22
4.1. INTRODUCTION.....	22
4.2. RESEARCH DESIGN AND METHODOLOGY.....	22
4.3. IRRADIATION AND ETCHING OF CR-39 DETECTORS.....	23
4.4. ETCHING PROCESS USING COLD PLASMA.....	23
4.5. DATA COLLECTION AND ANALYSIS.....	27
4.6. RESULTS AND DISCUSSION.....	28
PART 5.....	45
CONCLUSION.....	45
REFERENCES.....	46
RESUME.....	51

LIST OF FIGURES

	<u>Page</u>
Figure 2.1. (a, b, c, d) Shows images of the CR-39 tracer under a microscope, magnified at 40x magnification and for different exposure durations....	8
Figure 3.1. Radiation damage in (a) crystals (b) polymers	13
Figure 3.2. Stages of hidden track formation	14
Figure 4.1. Experimental setup.	24
Figure 4.2. Cold argon plasma optic emission spectrum lines.....	25
Figure 4.3. Cold helium plasma optic emission spectrum lines.....	25
Figure 4.4. Plasma power supply output signal waveform.	26
Figure 4.5. Argon and helium plasma thermal camera images.	27
Figure 4.6. Microscope used to detect antiquities.	28
Figure 4.7. Number of tracks with exposure time for Argon gas at a distance 3mm.	30
Figure 4.8. Number of tracks with exposure time for Argon gas at a distance 5mm.	31
Figure 4.9. Number of tracks with exposure time for Argon gas at a distance 7mm.	31
Figure 4.10. The Photo (a, b, c) represent the effects of argon plasma at a distance of 3 mm and at a time of 10 and 30 and 60 minutes.	32
Figure 4.11. The photo (a, b, c) represents the effects of argon plasma at a distance of 5 mm and at a time of 10 and 30 and 60 minutes.	33
Figure 4.12. Number of tracks with exposure time for Helium gas at a distance 3mm.	35
Figure 4.13. Number of tracks with exposure time for Helium gas at a distance 5mm.	36
Figure 4.14. The photo (a, b) represents the effects of Helium plasma at a distance of 3 mm and a time of 10 and 30 minutes.....	36
Figure 4.15. The effects of Helium plasma at a distance of 3 mm and a time 60 minutes.....	37
Figure 4.16. The photo (a, b) shows the effects of helium plasma at a distance of 5 mm and a time 10 and 30 minutes.	37
Figure 4.17. Shows the effects of helium plasma at a distance of 5 mm and a time 60 minutes.....	38
Figure 4.18. The correlation between results of chemical and plasma etching technique for Argon at D=3mm.....	38
Figure 4.19. The correlation between results of chemical and plasma etching technique for Argon at D=5mm.....	39

	<u>Page</u>
Figure 4.20. The correlation between results of chemical and plasma etching technique for Helium at D=3mm.	39
Figure 4.21. The correlation between results of chemical and plasma etching technique for Helium at D=5mm.	40
Figure 4.22. The relation between track density with distance at different times.	40
Figure 4.23. The fitting process for Argon gas at 3mm.	41
Figure 4.24. The fitting process for Argon gas at 5mm.	41
Figure 4.25. The fitting process for Argon gas at 7mm.	42
Figure 4.26. The fitting process for Helium gas at 3mm.	42
Figure 4.27. The fitting process for Helium gas at 5mm.	43
Figure 4.28. the diameter of the track with the exposure time for Argon gas at 3mm.	44
Figure 4.29. the diameter of the track with the exposure time for Helium gas at 3mm.	44

LIST OF TABLES

	<u>Page</u>
Table 3.1. Some types of inorganic reagents and their synthetic formulas.....	15
Table 3.2. Some types of organic reagents and their synthetic formulas.....	16
Table 4.1. Number of track with time at different distances for Argon gas.	29
Table 4.2. Number of tracks with time at different distances for Helium gas.	34
Table 4.3. The diameter of the track with the exposure time for each of the plasma.	43

SYMBOLS AND ABBREVIATIONS INDEX

SYMBOLS

Ar	: Argon
He	: Helium
NaOH	: Sodium hydroxide
KOH	: Potassium hydroxide
CO ₂	: Carbon dioxide
CH _x	: Chlorhexidine

ABBREVIATIONS

SSNTD _s	: Solid-State Nuclear Track Detector
AFM	: Atomic force microscope
DBD	: Dielectric barrier discharge
V-I	: Infrared dome
Le-D	: Light emitting diode
PM	: Particulate matter
NIST	: National Institute of Standards and Technology
UV	: Ultraviolet Index
DNA	: Deoxyribonucleic acid

PART 1

INTRODUCTION

Nuclear track detectors such as CR-39 are widely utilized in various fields including atomic physics, radiation dissymmetry, and environmental monitoring due to their high sensitivity, low cost, and ease of use [1]. CR-39 is a robust nuclear track detector made of a polymer material that demonstrates great potential for registering tracks of charged particles, and The CR-39 detector considered as one of the most widely used solid-state nuclear track detectors (SSNTDs.). It is a hydrocarbon composition, its molecular formula is $C_{12}H_{18}O_7$, and its density is 1.32 g/ cm^3 [1]. The percentages in its composition for oxygen, carbon, and hydrogen are 87.40%, 54.152%, and 56.6%, and its equivalent molecular weight is 274 [2]. as it possesses good qualities such as high optical transparency, homogeneity of its material, uniformity of properties, and high sensitivity to nuclear radiation such as alpha particles, protons, and fission products [3,4], in addition to its being unaffected by atmospheric factors when stored, as it does not dissolve in chemical solutions. The CR-39 decomposed by decreasing its thickness in the etching process [4, 5]. The detector has been adopt as a means of detecting alpha particles emitted from uranium, radon, thoron, and other isotopes that are found in food, air, and soil [6, 7].

The CR-39 detector is a polymer with an organic structure that contains carbon bonds in Monomer in the detector, and these bonds are relatively weak and break when radiation falls on them, which makes it more sensitive to radiation, especially when weaker bonds introduced into its lattice structure [4, 9]. The lowest energy of charged particles that the detector can sense is approximately 200 keV with normal chemical etching, and this value represents the minimum threshold energy of the detector [5]. The incident radiation acts on the detector (depending on the type of detector). For example, if it falls on polymers such as CR-39, it breaks the molecular bonds of the polymer through the process of expiation and ionization, which leads to

damage to the polymer. This damage reacts with alkaline solutions such as sodium hydroxide, which quickly penetrates the irradiated areas, causing visible tracks that increase in depth and expand in diameter with increasing etching time [10,12].

The researchers worked to find ideal conditions for the etching process with alkaline solutions. As an example for the CR-39 detector, a sodium hydroxide solution with a concentration or Normality of 6.25 is used and etching time of 5 to 7 hours and a temperature of 80°C [10,11,13]. The etching conditions can be change so that the etching time reaches 15 hours [12].

The scraping or etching process can be done, in addition to the chemical method, it can be a physical method that includes the same principle, which is melting the polymer that is exposed to radiation by using cold plasma. Cold plasma etching relies on plasma generated from ionized gases at low pressures to remove material from the substrate surface [14]. By applying high-frequency alternating current to the gas, plasma created containing highly reactive charged species like ions, electrons, and radicals [15]. These plasma species can interact with the polymer chains in CR-39, breaking bonds and etching away small molecules to select reveal the latent tracks over undamaged bulk material [16]. Compared to traditional chemical etching utilizing liquid etchants, cold plasma etching provides certain advantages for CR-39 track revelation.

Firstly, plasma can be generate at room temperature, eliminating the risk of thermal degradation associated with using hot corrosive acids.

Secondly, plasma parameters including gas composition, pressure, and power controlled precisely to optimize the etching performance. This permits finer control over etch rate, uniformity, anisotropy, and selectivity compared to chemical etchants. Thirdly, plasma etching precludes handling hazardous liquid chemicals, making it a clean and dry process. Finally, plasma can penetrate and etch narrow tracks and microscopic crevices with high resolution [17].

Overall, cold plasma etching enables selective revelation of latent tracks in CR-39 for various nuclear detection and dosimeter applications. Plasma conditions tune to match the track geometries and analysis requirements. However, some challenges remain regarding improving etching uniformity over large areas and comprehending the multifaceted plasma-polymer interactions [18]. Further research into this promising technique can help utilize its full potential for precise and well-controlled track etching in CR-39. Several research groups have studied the effects of key plasma parameters like power and gas flow rate on the etching outcomes of CR-39 detectors. However, the results have been inconsistent and sometimes contradictory. Hamid et al. reported that with increasing plasma power and gas flow rates, the number of revealed tracks rose. While the track radius reduced [19-20]. They found optimal conditions for high track density and well-defined shapes to be 40 W power and 30 sc/cm. In contrast, Hamid et al. observed negligible effects of power on tracks and radius, with only flow rate significantly influencing the outcomes [20]. At smaller distances, non-uniformity increases owing to localized effects while larger distances reduce plasma reactivity leading to slower etching [22]. It was determined the optimal distance to be around (3) mm for even track etching over the detector surface [23]. Pressure and treatment time are also critical for controlling etch rate, track clarity and detector thickness [24]. Several groups have also studied techniques to improve etching uniformity like rotating CR-39 under the plasma jet or using masks with regular perforations [25, 26]. Mixing heavier gases like Argon increases sputtering efficiency for revealing narrower tracks [27]. Modulating plasma properties using pulsed power sources or magnetic fields provides additional ways to control the etching mechanisms [28].

1.1. PROBLEM STATEMENT

In etching CR-39 detectors to reveal the tracks, the etching conditions, such as the plasma power and gas flow rate, can affect the number of tracks and the track radius, ultimately affecting the measurements' accuracy. Therefore, it is important to investigate the effect of these parameters on the etching process and optimize the conditions to obtain a high track density and well-defined track shape.

1.2. RESEARCH OBJECTIVES

The main objective of this study is to investigate the effect of cold plasma power and gas flow rate on the number of tracks and track radius in the CR-39 detector during etching. Specifically, the objectives are:

- To determine the optimal plasma power and gas flow rate for obtaining a high track density and well-defined track shapes.
- To analyze the relationship between the etching conditions and the number of tracks and track radius.
- To provide insights into the etching process of CR-39 detectors using cold plasma and optimize the process for various nuclear applications.

1.3. STUDY QUESTIONS

- How does the etching rate of CR-39 detectors vary with changes in the etching parameters such as power, gas flow rate, and pressure?
- How does the morphology of latent tracks in CR-39 detectors vary with changes in the etching parameters such as power, gas flow rate, and pressure?
- How does varying the irradiation dose affect the number, length, and diameter of latent tracks in CR-39 detectors?
- How does the etching process affect the sensitivity and accuracy of CR-39 detectors in detecting charged particles?
- What is the optimal combination of etching parameters that results in the highest quality and most accurate detection of latent tracks in CR-39 detectors?
- How does the effectiveness of cold plasma etching compare to other etching methods in revealing latent tracks in CR-39 detectors?
- How do environmental factors such as temperature and humidity effect the accuracy and reproducibility of the results?

1.4. SIGNIFICANCE OF THE STUDY

The relevance of this work rests in the possibility that it may increase the precision and reliability of data derived from CR-39 detectors. These detectors used in various sectors, including nuclear physics, radiation dosimeter, and environmental monitoring. This work has the potential to offer a safer and more environmentally friendly alternative to conventional techniques of etching by evaluating the influence of cold plasma power and gas flow rate on the etching process of CR-39 detectors and optimizing the settings. In addition, the findings of this research have the potential to contribute to the development of novel applications of CR-39 detectors in various industries. In general, the relevance of this work rests in the fact that it has the potential to expand knowledge of the process of etching CR-39 detectors and improve the performance of such detectors in a variety of nuclear applications.

PART 2

LITERATURE REVIEW

The result of the development of the use of nuclear trace detectors CR- 39 in many environmental, industrial and scientific applications, it has become necessary to improve the performance and work of the detector to detect alpha rays and ionizing particles (fission detector). Among these improvements are appropriate skimming conditions and the use of some physical methods to increase the efficiency of the detector. There for The most important recent research conducted in this field, including chemical method and physical method, which presented as follow:

- The efficiency of the CR-39 detector was studied as a function of etching time by Oliveira et.al (2021) using sodium solutions (NaOH), (KOH), and sodium hydroxide solution to which ethyl alcohol was added at temperatures of 70°C and 80° C. The track growth curve was drawn, and the diameter of the tracks measured at different etching conditions, including Temperatures. Different curves observed at 70°C and 80°C for etching times exceeding (6) and a half hours. The tracks density in the detectors was somewhat identical for both temperatures, 70°C and 80°C, and for the sodium hydroxide and potassium hydroxide solutions, with the exception of the sodium hydroxide solution with Ethyl alcohol, the tracks density decreased after (10) hours [29]
- Sahoo and his group (2014) used spectroscopy (Furrier transformation of infrared) and ultraviolet radiation to demonstrate the effect of irradiation with neutrons produced from bombarding Beryllium with different doses on the chemical and optical properties of the CR-39 detector. The results showed a linear increase in the absorbance of the detector with increasing dose. A practical relationship to neutron doses also deduced with these optical

properties, this technique is useful in calculating high doses, where the density of the effects is large and overlapping [30].

- Kravets et al. (2018) studied the surface and electrochemical properties of the thin polypropylene film treated with plasma, using nitrogen air and oxygen plasma. Through AFM images of the thin film surface, they showed that the precise topography of the thin film surface changes with the effect of etching, as the gaseous plasma leads to the formation of functional groups, the majority of which are carbonyl and carboxyl, in addition to the formation of polar groups that work. It improves membrane wettability, altering the thin film's electrochemical properties. It treated with plasma, which oxidizes the surface layer of the thin film. The effect of the treatment on the etching the surface of the detector and the increase in the diameter of the effect observe [31].
- In an important study, Hamid and his group (2016) used cold Argon plasma produced under conditions of normal atmospheric pressure in etching the polymeric CR-39 detector. The detector was irradiated with Radium-226 (^{226}Ra) source emitting alpha particles with an energy of (4.871) MeV and an activity of

(5 μCi). It was designed by the researchers and the appropriate working conditions were chosen for the experiment, such as the frequency (12) kHz and the potential difference of (6) kV, and the flow rate of 3L /min, and the time period was chosen from (5-50) minutes to expose the detectors to Argon plasma. The number of tracks per unit area calculate for each time period and the relationship was drawn for the density of the tracks with time, in addition to the relationship with the radius. The results showed an increase in the density of the tracks and the magnitude of the tracks, reaching their maximum value (8.49×10^4) track/cm², and the diameter of the track is (20) μm as a maximum value at a period of (20) minutes. The results of chemical etching using sodium Hydroxides (NaOH) with normality of (6 N) and etching time of (6) hours at a temperature of 80°C was (9.3×10^4) track/cm²[32] . Figure No. (1) show some pictures of plasma irradiation:

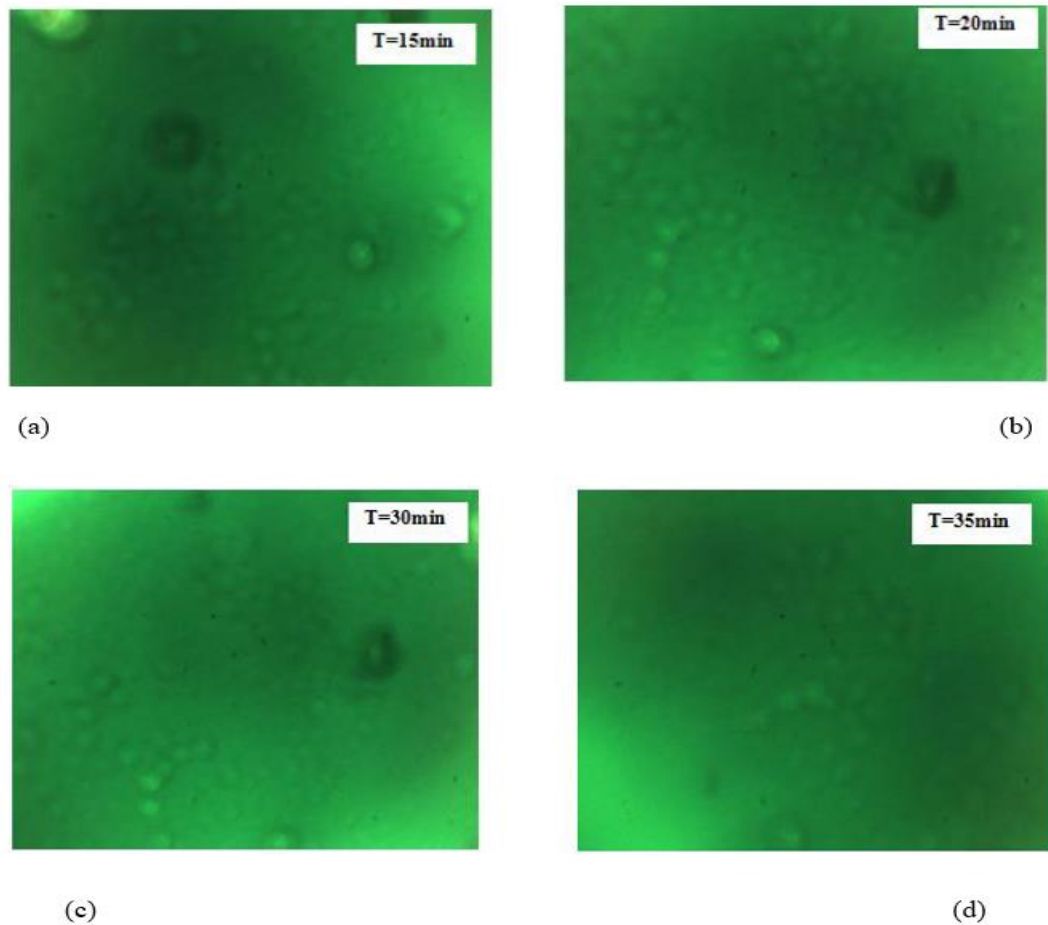


Figure 2.1. (a, b, c, d) Shows images of the CR-39 tracer under a microscope, magnified at 40x magnification and for different exposure durations [32].

A study about the unbalanced plasma under atmospheric pressure resulting from the dielectric barrier discharge (DBD) system carried out by Murbat and khudair (2014), to obtain the characteristic curves (V-I), the energy consumed and the breakdown voltage, glass with a thickness of one, two, and three millimeters was used as an insulator between the electrodes, and it was found that... The breakdown voltage in the experiment is at (1 Atom), where the pressure increases with the area of the gap and decreases with the frequency of the applied voltage. Accordingly, the researchers were able to generate a homogeneous and relatively cold plasma at atmospheric pressure [33].

Qasim and Al-Naimi in (2018) submitted a paper on finding the general etching rate V_B for a nuclear track detector type (LR-155) using the track length-diameter (L_e-D)

method, using a ^{241}Am source with activity of (1 μCi) and energy (5.485) MeV to irradiate the detector with different energies (1.8, 2.476, 3.46, 3.95) MeV. By changing the distance between the detector and the radiating source. The etching process for this detector done by using a (NaOH) solution using with normality of (2.5) N at temperature of 50° C. The results of the research indicated that the general etching rate V_B does not depend on the energy of the alpha particles, as it was calculated at different etching times [34].

In (2020), Manar and his group experimented with unconventional methods for etching different types of solid-state detectors, including CR-39 to obtain the most appropriate and best method for the etching of these detectors, which includes chemical etching, electrochemical etching, and the use of cold plasma to etched the (LR -115) and (PM -355) detectors. The CR-39 with different etching times and other requirements related to the use of chemical solutions and methods (like plasma). This study showed that the density of tracks for all techniques increased with the increase in the duration of exposure to the detector. The etching time has no relationship with the exposure time, so the greatest track density recorded by the CR-39 detector was at a period of exposed time of (15) sec was (14154) track/ mm^2 irradiated by ^{226}Ra source for different periods of time. While the microwave oven recorded (12976) track/ mm^2 , and the thermal oven recorded (1333) track/ mm^2 , and for the technique used cold plasma, the track density was (11660) track/ mm^2 . In general, the maximum sensitivity and efficiency of the three detectors at the highest exposure period (15) sec. was when they etched by plasma. Therefore, the researchers considered this technique to be the best among other physical techniques for all detectors [35].

Vettori and Abdullah (2016) investigated the effect of thermal annealing at various times on the behavior of Alpha particles recorded in the CR-39 detector, because this detector has a wide and large field of use due to its properties and advantages, such as ease of use, effect specialization, and the accuracy of the results obtained. Therefore, the researchers studied the process of annealing the detector under the influence of heat after it was irradiated with ^{241}Am source and compared the non-heat-treated reagents with those detectors that were treated using ultraviolet-visible

spectroscopy at a wavelength between (190–900nm). They also found that the energy gap for indirect transfer is less than the energy gap for indirect transition. In addition to changing the Urbach energy with an increase in the thermal annealing period, they also studied the effect of ultraviolet rays on the optical and recording properties of detectors, that is, the effect of these rays on etching rates and the sensitivity and efficiency of the detector when it was etched with a sodium hydroxide solution with a normality of (2.6)N. [36].

The CR-39 detector is widely used in environmental studies, especially measuring radon and thoron concentrations inside and outside buildings. Tan and his group in (2018) were interested in directing attention to working on studying the interaction of alpha particles with CR-39 detectors, explaining the physics of etching dynamics, and presenting the proposed basic theory for the purpose of improving etching conditions.

Measuring the concentrations of radon and thoron more accurately by studying the critical angle of incidence and the speed of general etching of the solution for the CR-39 detector [37].

Al-Jubouri, (2016) studied the effect of the concentration of the etching solution on the radius of the alpha particles tracks recorded by the CR-39 detector emitted from the ^{241}Am source, where the solution concentrations between (4 -10)N. for the purpose of devising a new experimental equation to describe the general etching rate as a function of concentration. The solution was found to be the optimal concentration at normality of (6 N), or through studying the sensitivity of the detector, which represents the highest value of the count at this concentration [38].

Ahmed Wathab in (2018) studied the properties of the nuclear tracks in CR-39 detector, when using two types of etching solutions. The first by dissolving sodium hydroxide in water only and the second by administering sodium hydroxide in water and ethanol at different temperatures of 70 °C and standard (5-8) with the addition of water only and at a temperature of 50 °C and standard. (3_15), When he adding water to ethanol after the detectors irradiated with an Am^{241} source with an energy of (5.48)

MeV for (20) seconds. The results showed an increase in the skimming rate V_B and the skimming rate V_T with the solution using the second solution, due to an increase in the activation energy of the skimming rate for this solution, but the sensitivity of the detector was greater when using the first solution [39].

In conclusion, etching is crucial for revealing the latent tracks left by charged particles in CR-39 detectors. There are several methods for etching CR-39 detectors, including wet chemical etching, electrochemical etching, and dry etching. Each etching method has advantages and disadvantages, and the choice of method depends on the specific application and desired track morphology. Cold plasma etching is a dry etching method that offers several advantages over wet chemical and electrochemical etching, including high precision, low damage, and environmental safety. However, optimizing the etching conditions and controlling the plasma parameters are important challenges that must be addressed to apply successfully cold plasma etching in various fields.

2.1. STUDY HYPOTHESIS

Hypothesis: Changes in the etching parameters, such as power, gas flow rate, and pressure, will result in variations in the morphology of latent tracks in CR-39 detectors.

Hypothesis: Increasing the irradiation dose will result in a higher number, longer length, and larger diameter of latent tracks in CR-39 detectors.

Hypothesis: The etching process will enhance the sensitivity and accuracy of CR-39 detectors in detecting charged particles.

Hypothesis: Cold plasma etching is more effective than other etching methods in revealing latent tracks in CR-39 detectors.

PART 3

THEORETICAL BACKGROUND

We have shown in the previous chapters that this research is important in order to dispense with the traditional methods of searching for traces, which we mentioned in some previous studies, and we found that our research to detect traces showed good results. This part will provide a general overview of trace detectors and non-thermal plasmas.

3.1. DETECTION PRINCIPLE

Solid materials that are electrically insulating used as tracks detectors; their specific resistances range from (10^6 - 10^{20} ohm.cm). Thin tracks known as latent tracks created when radiation charged particles like protons, alpha particles, and fission fragments passes through these detectors. This suggests that the tracks, or tracks, represent the amount of damage produced in the detector, which used to estimate the kind and energy of the falling particle [40].

When the kinetic energy of charged particles exceeds the energy required to excite the electrons or remove them from the valence band of the atoms of the substance with which they interact, the particles are able to ionized or excite the atoms [41, 42].

Mass appears to constantly lose energy as charged particles move through a medium due to a series of Columbic interactions with the electrons and forces of the medium, which cause continuous deceleration flows [43].

Most solid insulating materials, such as glass and polymers, are susceptible to radiation damage from charged particles. These particles can create narrow paths of radiation damage, such as atomic defects, crystal lattice gaps, and breaks in

molecular chains, also referred to as tracks, which are the result of particle damage in the atomic arrangement. Initially, these tracks appear as thin lines about 10 meters long. Micrometers, with dimensions of length $10\mu\text{m}$ and with $(50 - 100\text{\AA})$ and in the shape of tree branches [44]. As shown in Figure (3.1).

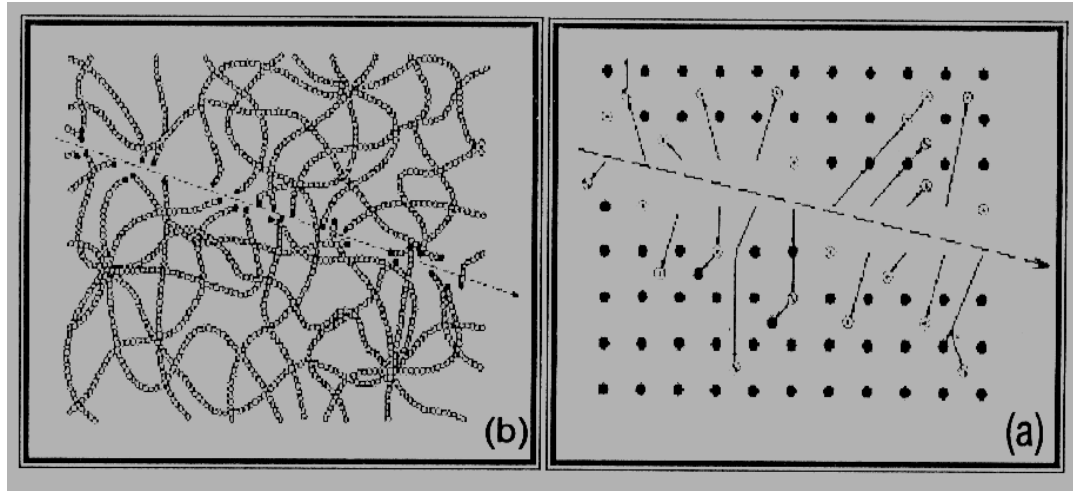


Figure 3.1. Radiation damage in (a) crystals (b) polymers [40].

The distance and speed of the charged particle determine the amount of energy it loses or causes ionization. During multiple collisions, the energy of the low-velocity particle disappears. [45].

It differs from high-energy fast particle interactions, where the majority of the energy is lost in the form of delta rays, which are secondary electrons emitted from the atoms of the reagent with sufficient energy to cause damage [46].

This enhances the amount of damage these electrons cause during their journey by causing more energy to be ionized or deposit. Although delta rays often contain high energy, their loss of energy causes radiation damage [47].

The ability to use the etching procedure to magnify the minimum damage density along the underlying paths, is a critical feature of solid-state detectors (SSNTDs) .

An important characteristic of solid-state detectors (SSNTD's) is the ability to expand the minimum damage density along the core of the trace by means of the etching technique [46]., as in Figure (3.2), which shows the stages of trace formation:

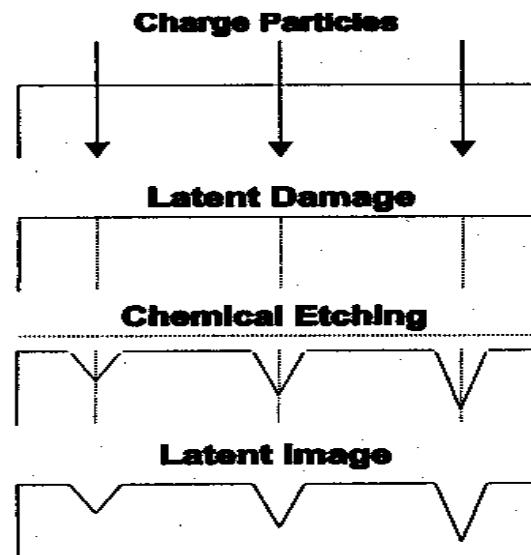


Figure 3.2 Stages of hidden track formation [46].

Damage caused by passing ionized particles can be observe using electron microscopy and small angle scattering (X-ray) [48]. These methods are accurate and very easy, but they are expensive and require special equipment. However, studies have proven the effectiveness of the chemical skimming technique. Drilling used to show traces in nuclear trace detectors due to its ease of use and the provision of abrasive solutions, in addition to its high effectiveness in enlarging traces to appropriate sizes that can be see under an ordinary optical microscope [48].

The abrasive solution (etching solution) applied to the damaged area, and allowed to attack and dissolve the material. The dissolved material then collected in the container containing the abrasive solution and reagent [49]. Depending on the components of the detectors, different solutions typically employed to etching tracks. Alkali metal hydroxides, including (KOH, NaOH), work well as organic reagent strippers [50].

Recent studies use a mixture of potassium hydroxide and sodium hydroxide in different quantities to improve the clarity and accuracy of the effect [51]. Hydrofluoric acid (HF) used as an inorganic reagent at specific concentrations and temperatures [40].

While one type of organic reagent is a polymer, which is a chemical compound consisting of several atomic groups linked together by chemical bonds to form long chains. When radiation breaks polymer chains into smaller chains (chain dissolution). The smallest forming unit of a polymer called a monomer [52].

3.2. REAGENT TYPES:

3.2.1. Inorganic Detectors

These compounds that lack hydrogen and carbon in their structure. Its atoms joined by ionic bonds. A few types of reagents and their synthetic formulae presented in Tables (3.1) [49].

Table 3.1. Some types of inorganic reagents and their synthetic formulas [49].

No.	Detector	Chemical Composition
1	Zircon	ZrSiO ₄
2	Quartz	SiO ₂
3	Mica (Biotite) Mica (Muscovite)	K(Mg.Fe) ₃ AlSi ₃ O ₁₀ (OH) ₂ KAl ₃ Si ₃ O ₁₀ (OH) ₂
4	Fluorite	CaF ₂
5	Soda Lime Glass	23SiO ₂ :5Na ₂ O:5CaO:Al ₂ O ₃
6	Olivine	MgFeSiO ₄
7	Calcite	CaCO ₃

3.2.2. Organic Detectors

These are substances made up of carbon, hydrogen, and oxygen. Because of the (C-C) and (H-C) bonds in them, which are easily broken by radiation, they have covalent bonds and are more sensitive than inorganic reagents. Furthermore, compared to organic reagents, organic reagents have a lower threshold energy and a

higher resolving power [47]. A few different reagent types and their synthetic formulae presented in Tables (3.1) [49].

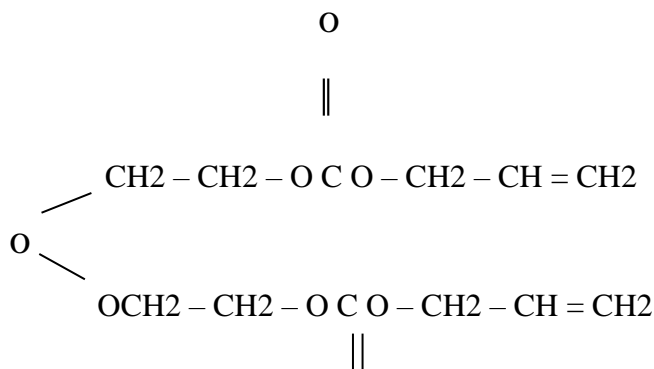
Table 3.2. Some types of organic reagents and their synthetic formulas [40, 49].

No.	Detector	Chemical Composition
1	Polyester (HBPAlT)	$C_{17}H_9O_2$
2	Polyimide	$C_{11}H_4O_4N_2$
3	Cellulose	
	Cellulose Nitrate	$C_6H_8O_9N_2$ (CN)
	Cellulose Triacetate	$C_3H_4O_2$ (CT)
4	Plexiglass	$C_5H_8O_2$
5	Polycarbonate (Lexan, Makrofol)	$C_{16}H_{14}O_3$ (PC)
6	Polylyldiglycol Carbonate	$C_{12}H_{18}O_7$ (CR-39)

3.3. POLYMER NUCLEAR TRACK DETECTOR CR-39

It is one of the organic nuclear track detectors. its molecular formula is ($C_{12}H_{18}O_7$). It has the symbol CR (Columbia Resin), and it discovered by three researchers.

(Cartwright, Shirk & Price) in 1978 at the University of California, USA [56] and was manufactured in the same year [98]. Its trade name is CR-39. It made by polymerizing a liquid monomer with a hydrocarbon composition ($C_{12}H_{18}O_7$) [55]. Its chemical composition is.



3.4. SOME SKIM EFFECT COEFFICIENTS

3.4.1. Rate of Bulk Etch (V_B)

The amount of material that removed from the surface of the detector during the chemical etching procedure. (V_B) is a function of standard (concentration) and temperature V_B (N, T), depending on the reagent and skimming conditions, which include temperature and solution type and concentration. It can be determined by multiplying the abrasion time (t) by the thickness of the layer removed (h) [51] where :

$$V_B = h/t \quad (3.1)$$

3.4.2. Track Etch Rate V_T

It is the speed of scraping the trace along the path of the particle [37]. V_T depends on the type and energy speed of the falling particle, in addition to the temperature and concentration of the abrasive solution.

Both the skimming equations (V_B) and (V_T) affected by temperature changes and the type of relationship is an exponential relationship. The researchers Hunyadi and Simonyi =introduced the effect factor of the concentration of the skimming solution, and the relationships were [55]:

$$V_B = f_B C^{n_B} \exp(-E_B/KT) \quad (3.2)$$

3.4.3. Etching Rate Ratio V

It is the ratio between the speed of scraping the trace to the speed of scraping the surface of the detector, represented by the following relationship [40]:

$$V = V_T / V_B \quad (3.3)$$

3.4.4. The Critical Angle θ_c

The critical angle is the minimum angle at which the effect hidden by abrasive solutions can be reveal and it given by the following relationship [49]:

$$\theta_c = \sin^{-1} V_B / V_T \quad (3.4)$$

3.4.5. Efficiency of the Detector to Record the track) η)

It is the ratio between the number of traces recorded by the detector to the number of particles falling on the detector [49], and it given by the following relationship:

$$\eta = 1 - (V_B / V_T) \quad (3.5)$$

$$\eta = 1 - \sin \theta_c \quad (3.6)$$

3.5. COLD PLASMA

Along with solids, liquids, and gases, plasma is a unique fourth state of matter that was identified in 1879 by physicist William Crocks and dubbed ionized gas by Dr. Iron Langmuir in 1929[58].

Vacuum plasma technology is another name for low-pressure cold plasma technology.

A partially ionized gas called plasma produced by giving it energy in the form of heat, radiation, or electricity. The primary attributes and other fundamental elements of cold plasma define its temperature, which varies between 30 °C and 50 °C. Cold plasma said to be the most commonly employed for medicinal applications because of its low temperature and sensitivity, which allow it to produce gases like nitrogen and oxygen that used in medicine [59].

3.6. COLD PLASMA IS CREATED

Electrical discharge in low-pressure gases produces low-temperature plasma. They consist of a variety of highly reactive substances, including radicals, ions, electrons, photons, and excited molecules. Device factors, such as chamber shape, gas flow rate, frequency, and applied power, determine its physical and chemical composition as well as the gas used. By applying this technique, the chemistry and morphology of polymer surfaces can be change down to several tens of microns, essentially maintaining their macroscopic properties. Thus, it is possible to achieve completely distinct chemistry, hydrophobicity, or surface roughness.

The scientists concluded that the etching was mostly due to ion bombardment and that neutral species acting on the surface of the plasma-activated polymer were mainly responsible for the surface chemical changes [60].

By using radio frequencies or microwaves to excite gas molecules and create charged molecules (free radicals), gaseous plasma created. The mechanisms used in the gaseous plasma process combine the effects of oxygen free radicals and light (UV) produced by excited molecules.

Microorganisms suffer damage to their (DNA) strands due to ultraviolet light. (UV) photons cause photo absorption internally, disrupting chemical bonds with other compounds in microorganisms to produce volatile byproducts such as (CO₂) and (CH_x). Atomic and molecular radicals, as well as molecules excited in a metastable state, are reactive species in the plasma field that react chemically with cell components to stimulate autophagy, perturbing microorganism structure and metabolism and producing final oxidation products such as carbon dioxide [61].

3.7. GAS HELIUM

Helium is an extremely light, tasteless, colorless, and odorless noble gas with a wide range of uses and a good safety record does not facilitate burning. It is distinct from the other elements in that it has the lowest melting and boiling temperatures (−458

°F), (−272.2 °C) and (−452.1 °F) (−268.9 °C). The second most common element in the universe is helium. The majority of the helium needed taken during the production of natural gas since it is a byproduct of radioactive decay underneath. Certain features of helium, such as its low density, poor solubility, and strong thermal conductivity, are necessary for certain applications. Two-thirds of the helium utilized or (7,000) tones, is used to cool superconducting magnets in magnetic resonance imaging (MRI) machines. Despite being referred to as the lifting gas in balloons and blimps less than (7%) of utilization is for this purpose.

The lightest noble gas is helium (4 g/mol). Hydrogen is the only gas having a density less than that of helium.

Because of its unique physical and chemical characteristics, including as its low density, poor solubility, and high thermal conductivity, the noble gas helium has a wide range of uses. The vast majority of helium-related medical research focuses on how it might be used as adjuvant therapy for a variety of respiratory conditions, including bronchiolitis, acute respiratory distress syndrome, chronic obstructive pulmonary disease, croup, and asthma flare-ups. It has recently been demonstrate that helium gas, which was previously believed to be physiologically inert, actually helps to prevent myocardial ischemia through a number of different processes [62].

3.8. USING COLD PLASMA TO SANITISE SURFACES

In the first biomedical use, plasma gases utilized to disinfect surfaces and remove pollutants and toxins using cold plasma. It shown that utilizing 1% oxygen mixed with cold plasma of argon gas works better at eliminating traces and cluster deposits from surfaces [63].

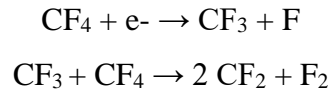
Cold plasma surface treatment is a superior technique because it uses a modified procedure that requires no additional initiator or solvent and produces less pollution, takes less time to complete, requires simple equipment to operate, is highly efficient, and is extremely safe. Two reasons explain why plasma treatment increases the tensile strength of fibers: Firstly, the surface treatment of plasma only affects shallow

surfaces; the body strength is unaltered. Furthermore, surface cracking will totally eliminated by slow plasma etching, which will decrease the source of stress concentration and hence raise the tensile strength of the fibers [64].

3.9. DRY ETCHING

Dry etching methods, such as cold plasma etching, have gained increasing attention due to their high precision, low damage, and controllability. Cold plasma etching involves using plasma generated by low-pressure gases to remove material from the detector selectively.

Dry etching using a plasma generated by CF₄ gas:



In this equation, a low-pressure gas such as CF₄ generates plasma. The plasma reacts with the CR-39 polymer to produce volatile products, which removed from the surface of the detector. The specific reactions will depend on the type of gas used and the plasma conditions [28].

However, some limitations and challenges are associated with cold plasma etching. One of the challenges is optimizing the etching conditions, which can be affect by various factors such as plasma power, gas flow rate, and gas mixture. The optimal etching conditions may depend on the specific material and the desired track morphology. Another challenge is the control of the plasma parameters, which can affect the etching rate and track morphology. The plasma parameters can be affect by various factors such as chamber pressure, gas composition, and power supply [57].

PART 4

METHODOLOGY

4.1. INTRODUCTION

The study aims to investigate the effectiveness of cold plasma etching for revealing latent tracks in CR-39 detectors created by alpha particle irradiation. The latent tracks left by charged particles passing through the CR-39 material can provide valuable information about the energy and direction of the particles, making it an essential tool in various fields such as particle physics, radiation dosimeter, and space science.

The methodology involves a controlled laboratory experiment conducted in a particle accelerator facility. The experiment included irradiating CR-39 detectors with charged particles that emitted from different sources and preparing the detectors for etching using cold plasma. The etching process parameters optimized, such as power, gas flow rate, and pressure, which can be varied to investigate their effects on the track morphology and etching rate.

4.2. RESEARCH DESIGN AND METHODOLOGY

The research strategy for this study uses a carefully monitored experiment carried out in a laboratory setting. The experiment starts with irradiating CR-39 detectors with charged particles. After that, the detectors prepared for the etching process by utilizing cold plasma. The etching process settings will be change to evaluate the effects of these changes on the track morphology and the etching rate. The experiment carried out on several occasions to guarantee the dependability and validity of the findings.

4.3. IRRADIATION AND ETCHING OF CR-39 DETECTORS

The first stage in this approach is irradiation of CR-39 detectors with alpha particles that emitted from ^{241}Am with energy of 5.48 MeV in contact with the detector. The detectors positioned under the plasma with different heights, at different exposure times. The particles' energy and flow will be under close control to maintain the uniformity and reproducibility of the irradiation dosage.

In this experiment, CR-39 nuclear track detectors were exposed to plasma at distance (3,5, and 7 mm) for Argon plasma, and (3,5 mm) for Helium plasma. Time intervals (5, 10, 20, 30, 40, 50, and 60 minutes) for Argon plasma and (5, 10, 20, 30, 40, 50 minutes) for Helium plasma.

The subsequent procedure in the approach is preparing the detectors to be etched with cold plasma to go on to the next stage. To eliminate any potential surface contamination from the detectors. After that, Distilled water used for cleaning the detectors, and dry air will be used to dry them to remove the moisture from the detectors and completely.

4.4. ETCHING PROCESS USING COLD PLASMA

The etching procedure will be carry out with a cold plasma machine, which included many components like a power supply, a gas distribution system, and a vacuum chamber. A turbo-molecular pump will bring the pressure within the vacuum chamber to a low of (2-10) Torr. The etching gas will be introduce into the chamber through the gas delivery system, which will be regulate to obtain the required gas flow rate and pressure.

The optimize values for plasma system was the same for both plasma types (Argon and Helium) flow rate with (3 L/min). The operating voltage was set at (12) kV and the frequency at (10) kHz. In this work, the irradiated detectors then exposed to argon and helium plasma for limited time intervals and at different distances. We can observe the experimental setup from Figure (4.1):

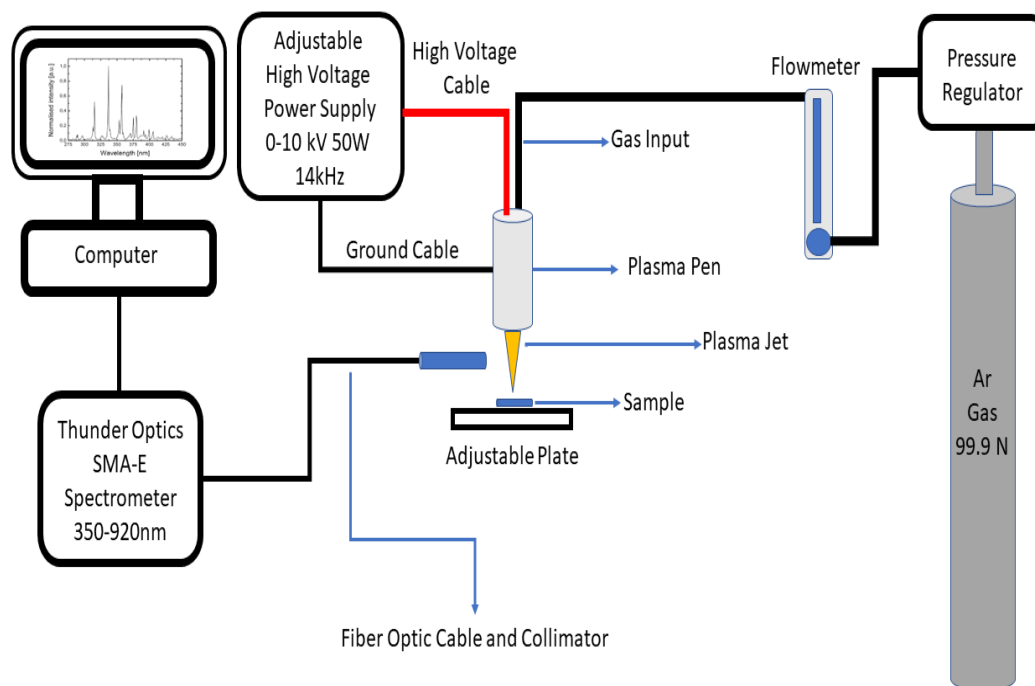


Figure 4.1. Experimental setup.

A Thunder Optics model (SMA-E) and optical emission spectrometer with a wavelength measurement range (350-920) nm were used to perform optical emission analysis of cold argon plasma obtained at atmospheric pressure. To obtain high-resolution results during plasma formation, the fiber optic cable placed at a distance of 1 cm to see the center of the plasma jet. The emission line graph for both argon and helium gases obtained after converting the results from the spectrometer into a graphical form. The graph of the figures (4.2) and (4.3), the emission lines of argon and helium appear at different wavelengths. Argon I and II. The degree of helium ionization values was determined. (NIST) Atomic Spectra Database used to identify emission lines.

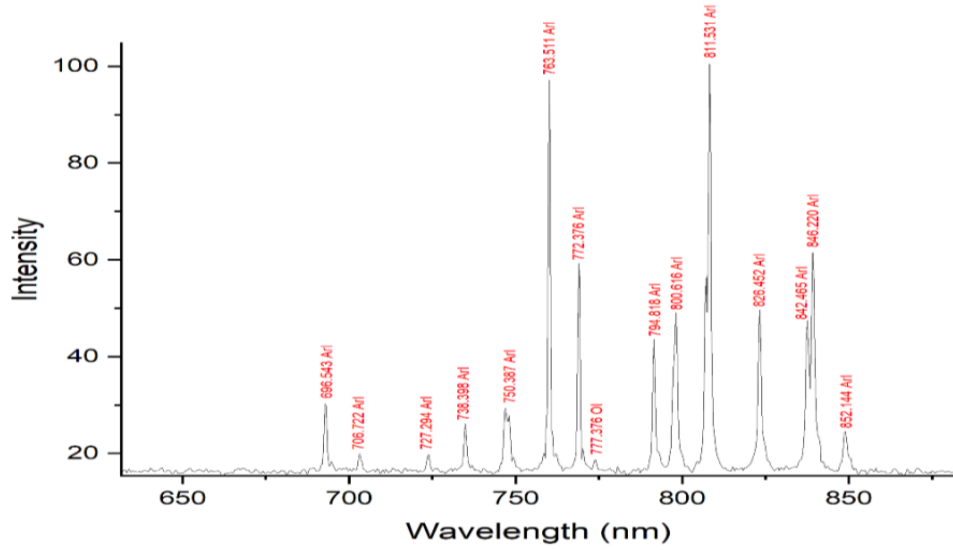


Figure 4.2. Cold argon plasma optic emission spectrum lines.

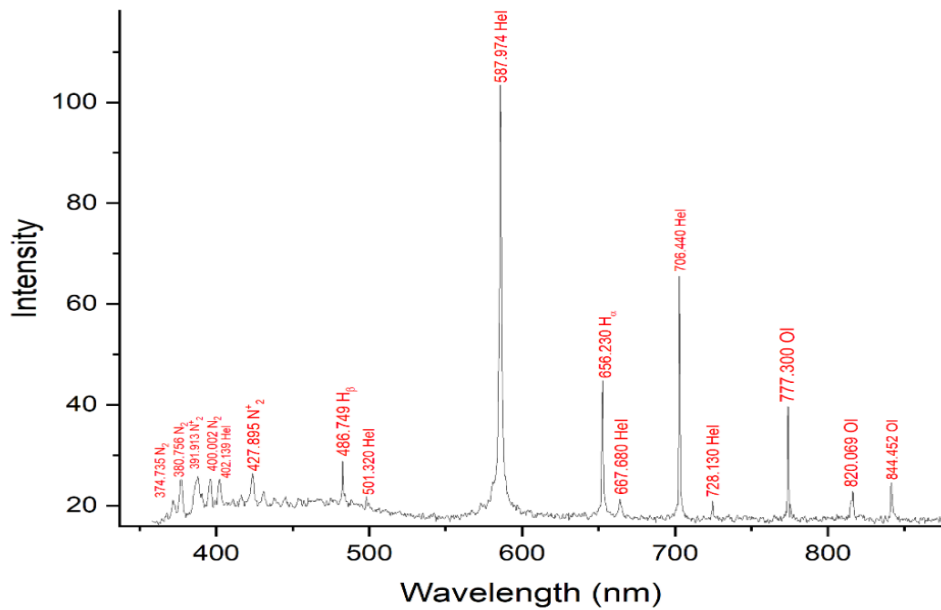


Figure 4.3. Cold helium plasma optic emission spectrum lines.

To generate a plasma, the power supply will be connect to a high-frequency alternating current that will be apply to the gas inside the chamber. The plasma will produce highly reactive species such as ions, electrons, and radicals, which will react with the detector surface and induce selective removal of the material around the latent tracks. These reactions will take place because the plasma is very reactive. To explore how the plasma's power, gas flow rate, and pressure affect the etching rate and track morphology, the characteristics of the plasma, such as power and gas flow

rate, will be change Figure (4.4) shows an oscilloscope image of the signal applied to the electrodes at the moment of plasma formation using a high voltage probe.

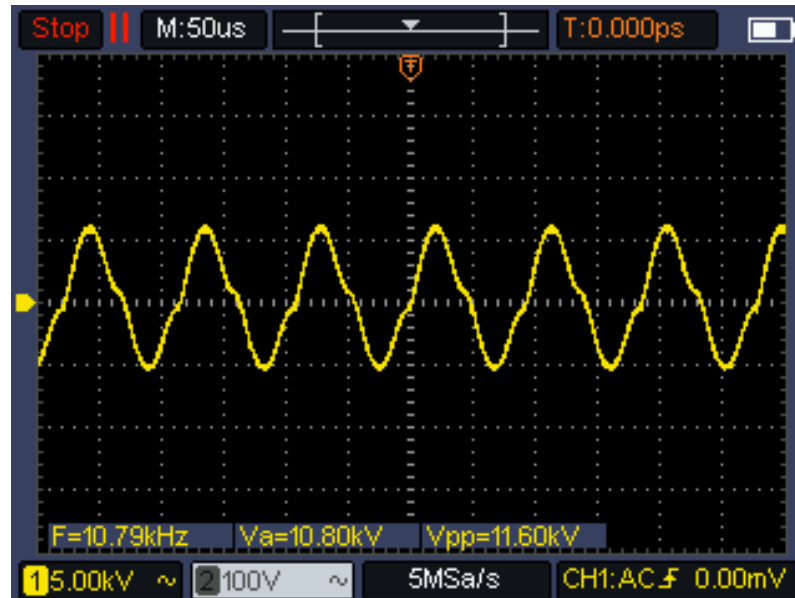


Figure 4.4. Plasma power supply output signal waveform.

In Figure (4.5) the temperatures generated on the surface by helium and argon plasma were visualized with the help of Seek XR model thermal camera. After long-term application, surface temperatures measured as 42°C for helium plasma and 43°C for argon plasma.

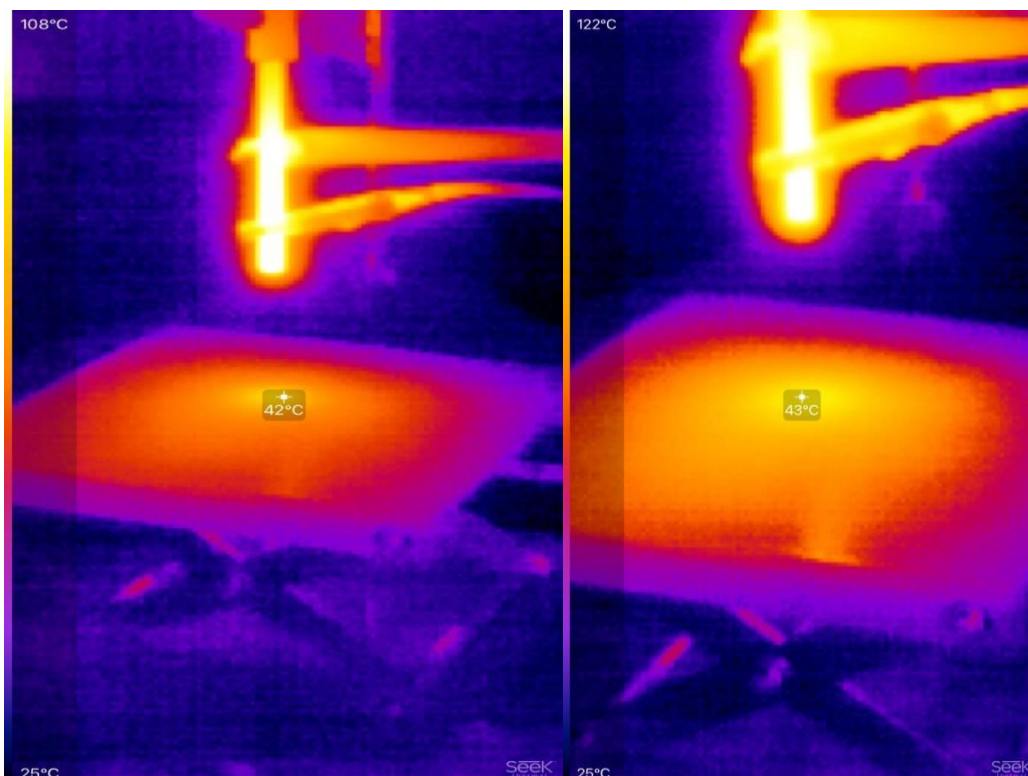


Figure 4.5. Argon and helium plasma thermal camera images.

4.5. DATA COLLECTION AND ANALYSIS

The last stage in this work was determining the number of tracks in detectors using an optical microscope (ANOVA) type (ZoomexXSP-44SM) with a magnification of 400X to get radon concentration, using statistical techniques for ten attempts to get the average. The figure (4.6) shows the microscope that used during the experiment:



Figure 4.6. Microscope used to detect antiquities.

4.6. RESULTS AND DISCUSSION

By observing Table No. (4.1) of the values of counting tracks of alpha particles in the CR-39 detector, which were recorded at exposure distances to argon gas plasma (3,5, and 7) mm and with time periods (5,10,20,30,40,50, and 60) minutes. We find that the count value of tracks increases with increasing of the time period of exposure to plasma until it reaches the highest value at the period of 40 minutes, which are (3444.773, 3616.042, and 2877.554 track/mm²) at distances of (3,5, and 7) mm, respectively, as shown in Figures (4.7, 4.8, and 4.9) of Argon gas. This study aimed to evaluate the effectiveness of helium plasma etching compared to the established argon plasma method for track recognition of alpha particles in CR-39 detectors. The recognition achieved with helium plasma was comparable to the reference method employed by [Dr. Hamid]. As illustrated in(Table 4.2), the number of alpha particle tracks detected increased with increasing exposure time periods at both (3 mm and 5 mm) exposure distances to helium gas plasma. The highest track densities were observed at (40 minutes) of exposure, reaching (6081.525 tracks/mm²) and

(4963.525 tracks/mm²) for distances of (3 mm and 5 mm), respectively. These results, along with Figures (4.20 and 4.21), suggest that helium plasma can be a viable alternative to argon plasma for the etching process of CR-39 detectors, as demonstrated in Figures (4.10, 14, 15, 16, 17). Furthermore, Figures (4.18, 4.19, 4.20, and 4.21) depict the relationship between the track counts obtained after chemical etching and the difference values between these counts and those achieved with plasma etching. Interestingly, an initial inverse correlation was observed. Additionally, track counts recorded using helium plasma were higher than those obtained with argon plasma, and the correlation coefficient for helium plasma was stronger. Where the correlation coefficient for Argon plasma was ($r = 0.712467$) at a distance of (3) mm as in Figure (4.18), and ($r = 0.631714$) at a distance of (5) mm as in Figure (4.19). As for helium gas, it was ($r = 0.876317$) at a distance of (3) mm, as in Figure (4.20), and ($r = 0.862396$) at a distance of (5) mm, as in Figure (4.21). The difference could be due to the temperatures of each of the two types of plasma, as it is 38°C and 43°C for helium. And from Figure (4.22) for the values of counting tracks with distance (3,5, and 7) mm for time periods (5,10,20,30,40,50, and 60) minutes, where we find the relationship is inverse for each time period with the effect of plasma with increasing distance. Therefore, expect it with helium gas and the clear effect through Table (4.2)

Table 4.1. Number of track with time at different distances for Argon gas.

Time (min)	Number of tracks(tracks/mm²)		
	D=3mm	D=5mm	D=7mm
5	1808.021	1150.558	986.336
10	2136.752	1314.924	1106.428
20	2958.579	1643.655	1369.275
30	3451.676	3459.676	2641.956
40	3944.773	3616.042	2872.554
50	3451.676	2794.214	2594.216
60	2958.579	2301.117	1952.183

Table 4.1 presents data on the number of tracks per mm² revealed in a CR-39 nuclear track detector after cold plasma etching for different etching durations and at different distances between the plasma nozzle and detector surface. Argon gas used for plasma generation.

Several observations can be made from the trends in the track density data. Firstly, for a given nozzle-to-surface distance, the number of revealed tracks consistently increases with increasing etching time from (5) to (40) minutes. This indicates that prolonged plasma exposure etches deeper into the CR-39, revealing more latent track. The increase is steep up to (30) minutes after which it starts plateauing.

Secondly, for a given etching duration, the track density markedly decreases as the nozzle-to-detector distance increases from (3mm) to (7mm). The plasma species have the highest flux and energy, resulting in greater etching and higher track revelation. As the distance increases, the flux and reactivity reduce, leading to lower etching efficiency.

Finally, the track density reaches a maximum value between (30-40) minutes for all distances. After (40) minutes, the track density starts decreasing for longer etching durations. A likely explanation is that for extended exposures beyond (40) minutes, erosion of the detector surface begins to dominate over selective etching of tracks, ultimately destroying the revealed tracks.

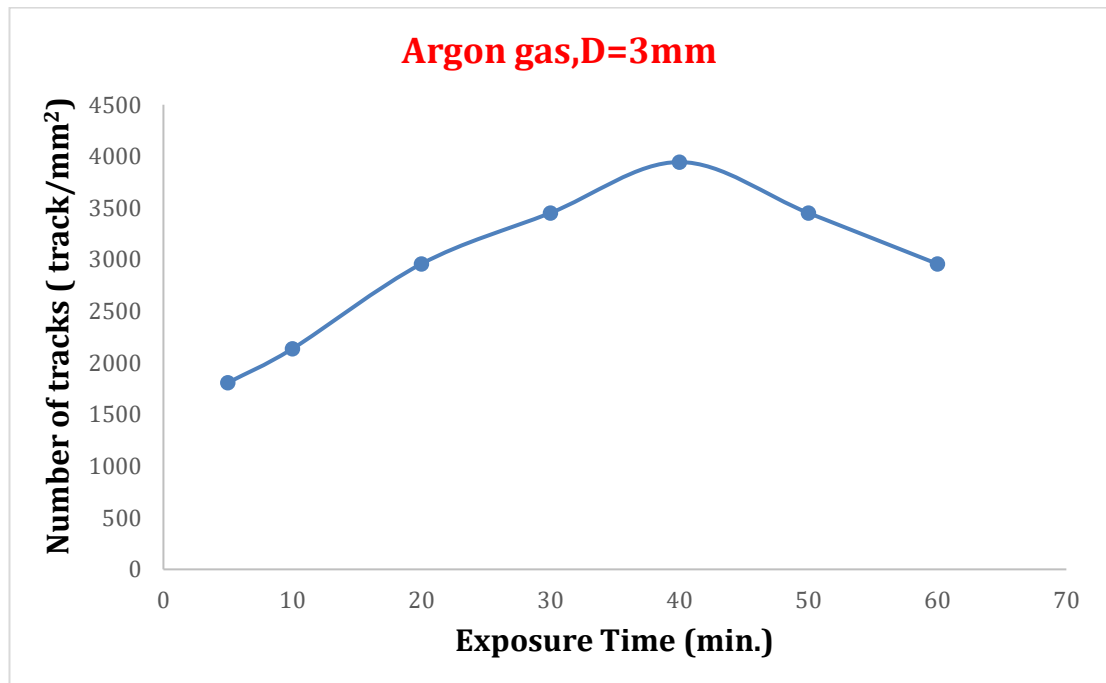


Figure 4.7. Number of tracks with exposure time for Argon gas at a distance 3mm.

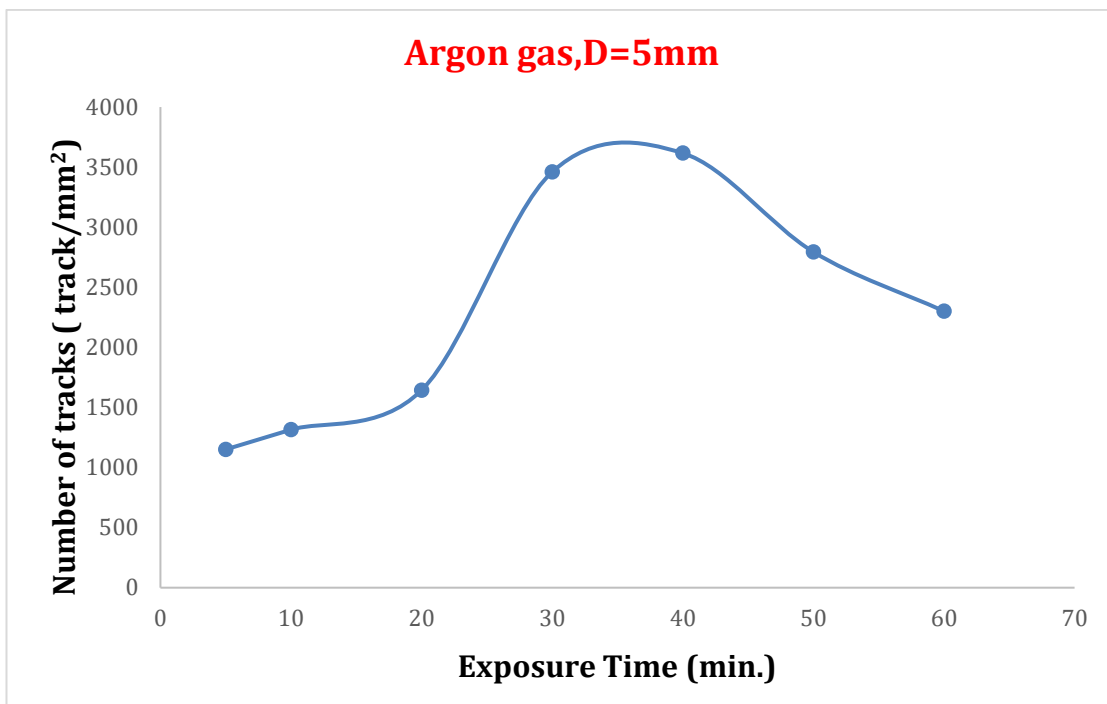


Figure 4.8. Number of tracks with exposure time for Argon gas at a distance 5mm.

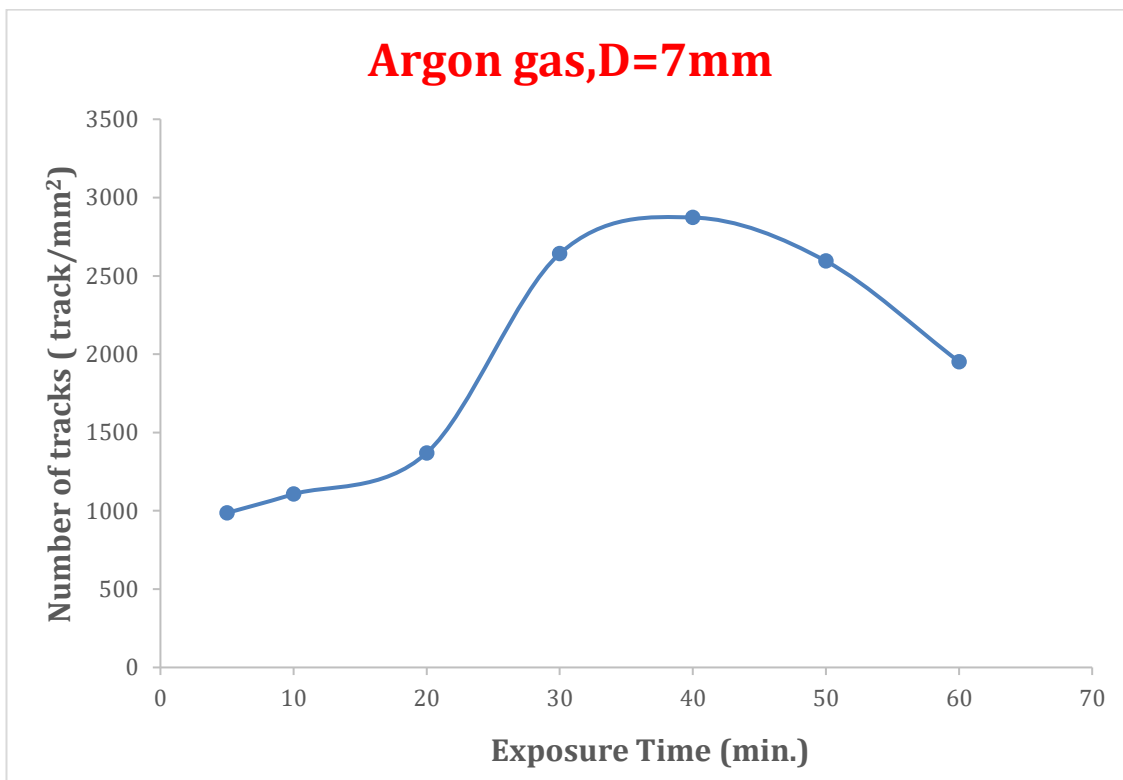


Figure 4.9. Number of tracks with exposure time for Argon gas at a distance 7mm.

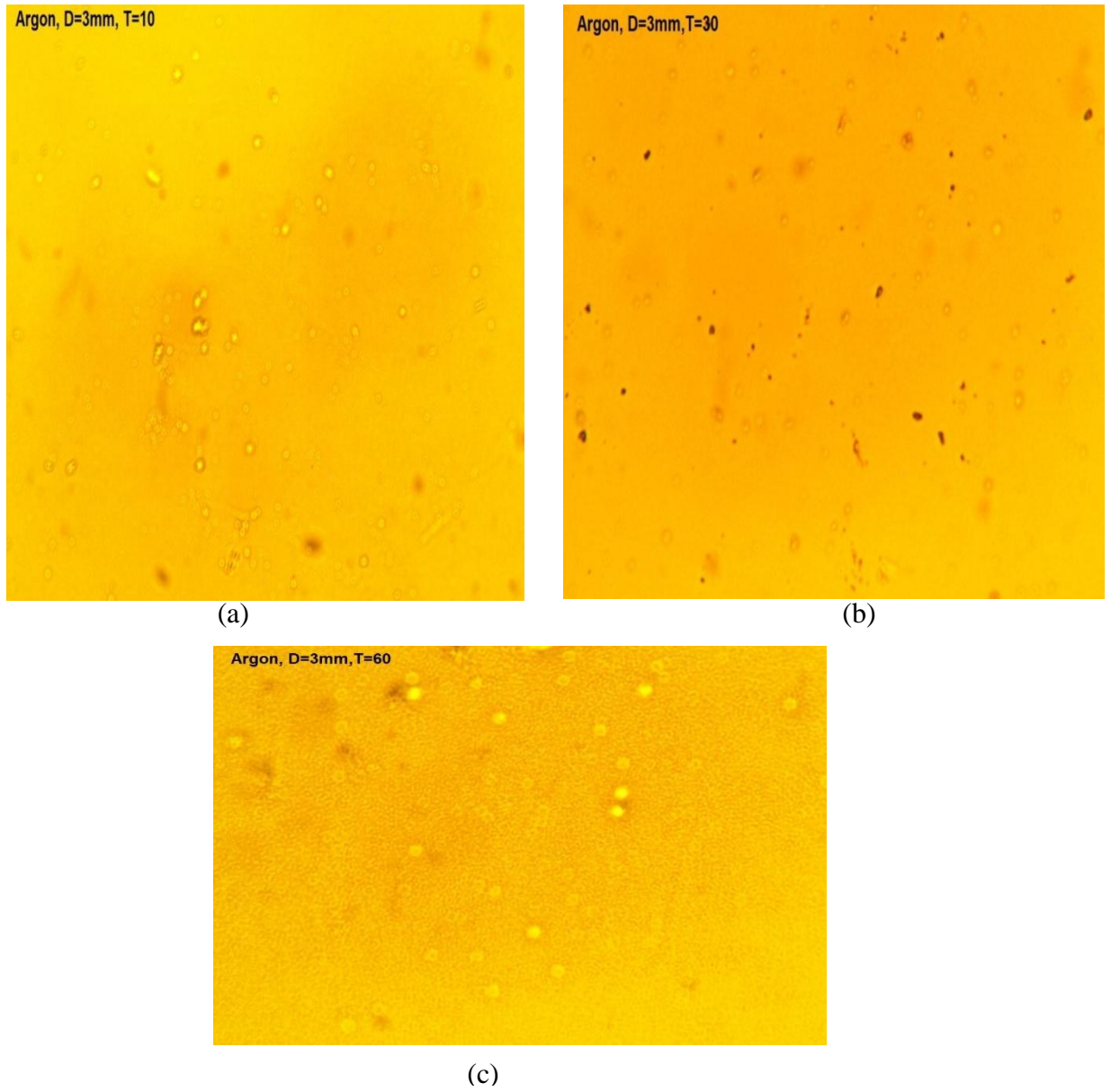
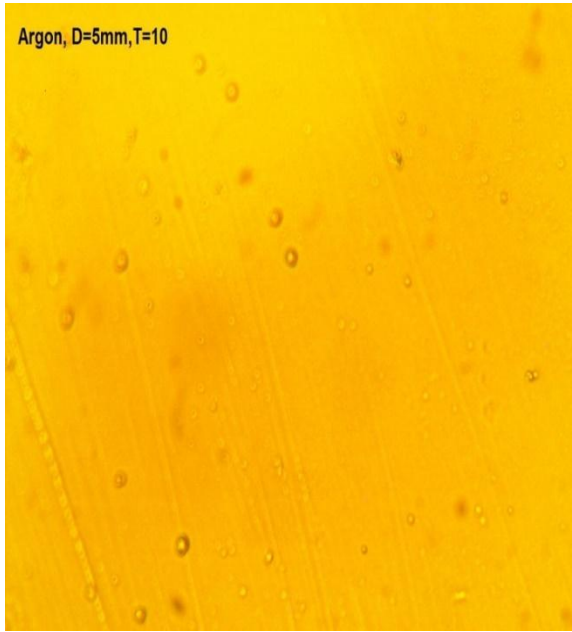


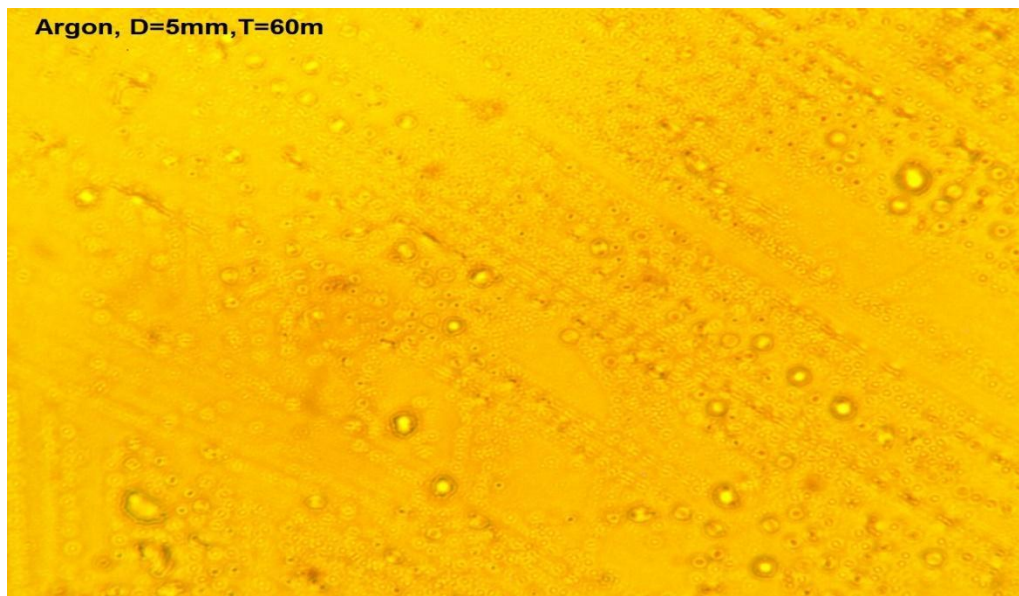
Figure 4.10. The Photo (a, b, c) represent the effects of argon plasma at a distance of 3 mm and at a time of 10 and 30 and 60 minutes.



(a)



(b)



(c)

Figure 4.11. The photo (a, b, c) represents the effects of argon plasma at a distance of 5 mm and at a time of 10 and 30 and 60 minutes.

Table 4.2. Number of tracks with time at different distances for Helium gas.

Time (m)	Number of tracks(tracks/mm ²)	
	D=3mm	D=5mm
5	1643.655	1808.021
10	2301.117	2301.117
20	3105.483	3122.945
30	3944.773	3854.138
40	6081.525	4963.525
50	5259.697	4273.304
60	4602.235	4188.697

(Table4.2) presents data on the number of tracks per mm² revealed in a CR-39 nuclear track detector after plasma etching using helium gas. The etching was conducted for different durations ranging from (5) to (60) minutes and at two nozzle-to-detector distances of (3) mm and (5) mm.

The key observation from the track density data is that the number of revealed tracks shows an increasing trend with etching time for both (3) mm and 5mm distances. This indicates continuous etching of the latent particle tracks in the CR-39 detector by the helium plasma as the exposure time is increased. However, the rate of increase reduces progressively after (40) minutes for 3mm and after (50) minutes for (5) mm distance.

Comparing the two nozzle-to-detector distances, the track density is slightly higher at (3) mm than (5) mm distance for any given etching duration. This can be attribute to the higher flux and reactivity of plasma species at shorter distances from the source, resulting in more effect etching.

An interesting difference seen in the etching time corresponding to the maximum track density for the two distances. The peak track revelation occurs at (40) minutes for (3) mm distance, while it continues to increase until (50) minutes for the (5) mm distance. This suggests the optimal etching duration is dependent on the source-to-sample gap.

Moreover, in contrast with argon plasma etching, the revealed track density does not decrease but plateaus after the peak etching time. This indicates that helium plasma

etching has better selectivity in revealing tracks without significantly damaging them even after prolonged exposure.

Figures (4.23,24,25,26 and 27) show the results of fitting process for all data, which are most of them are fifth degree that means etching by using plasma have the same behavior, and we can the suitable one for etching.

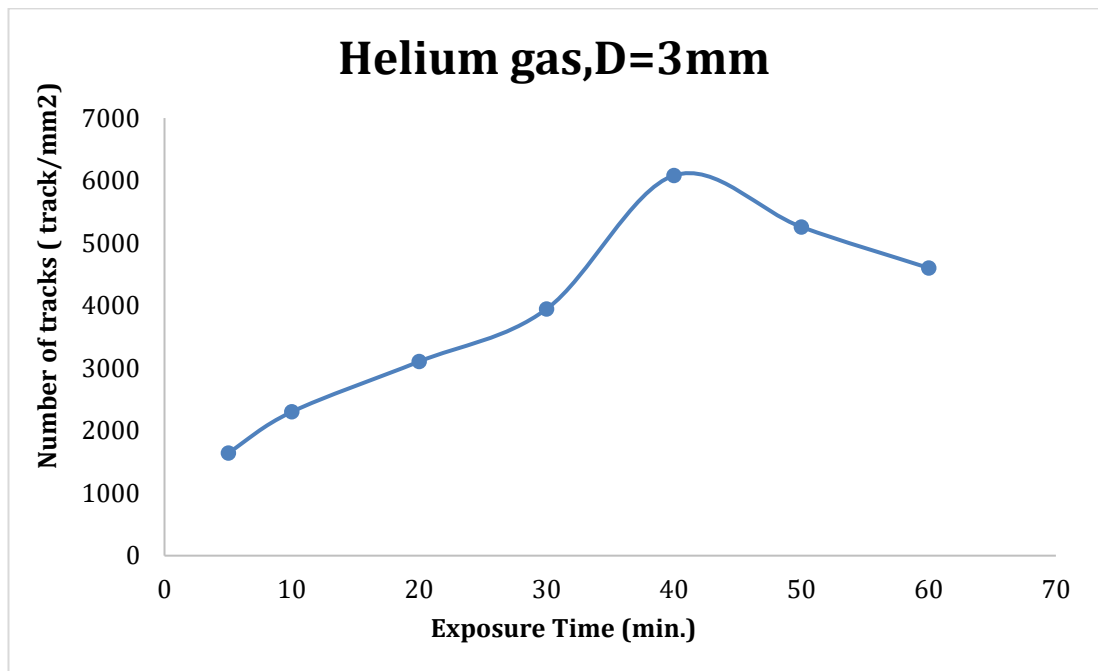


Figure 4.12. Number of tracks with exposure time for Helium gas at a distance 3mm.

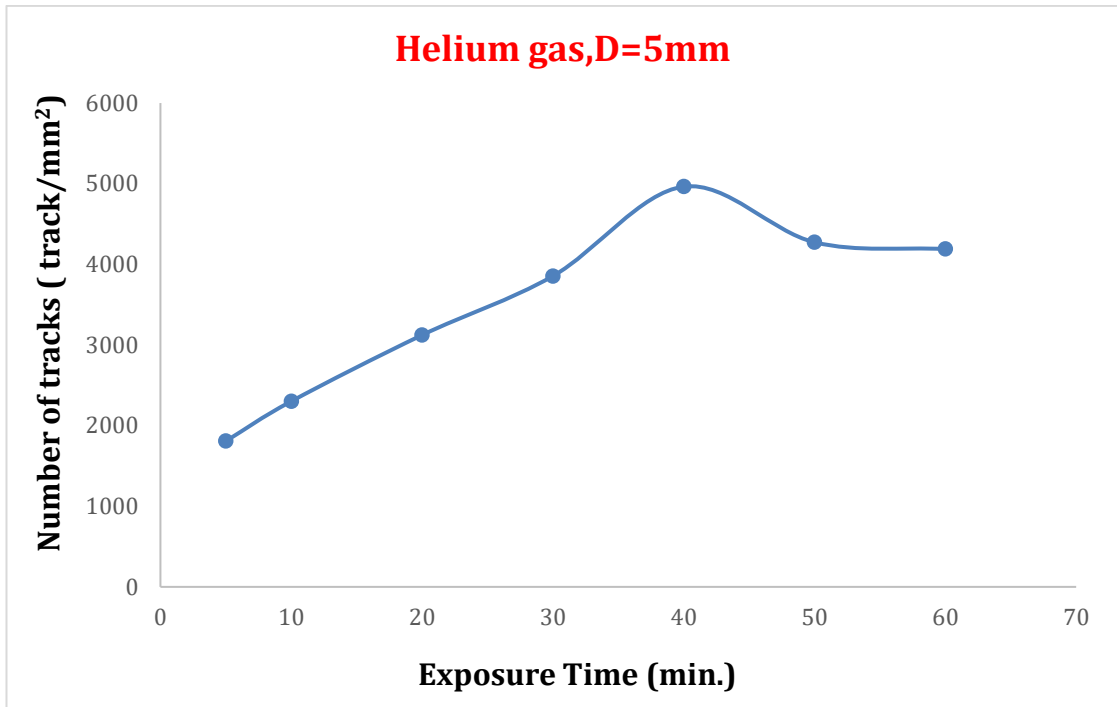


Figure 4.13. Number of tracks with exposure time for Helium gas at a distance 5mm.

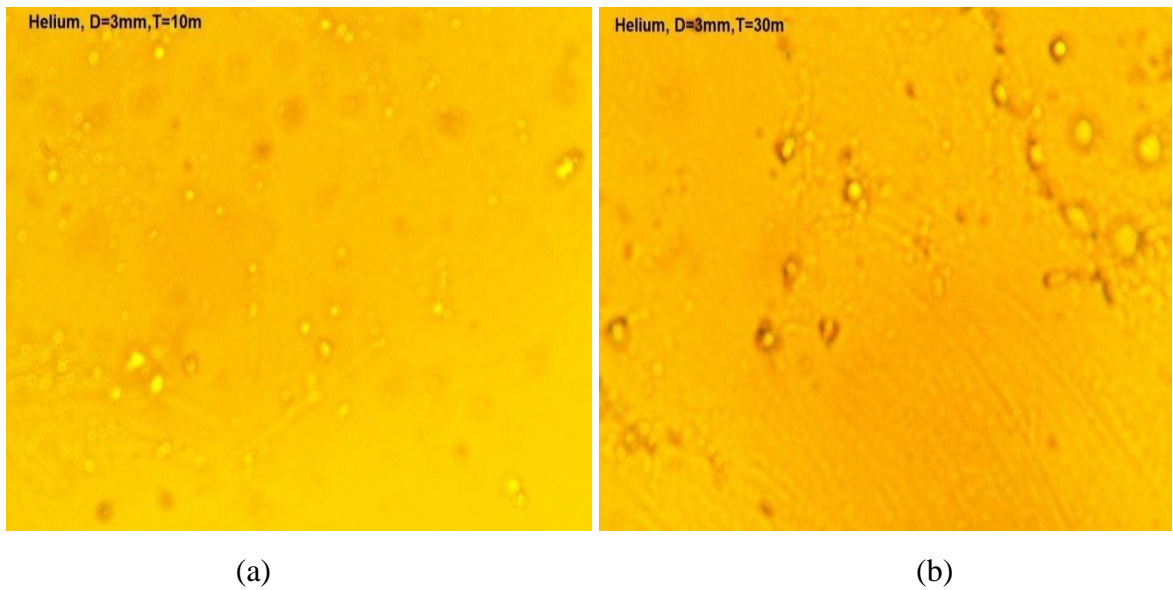


Figure 4.14. The photo (a, b) represents the effects of Helium plasma at a distance of 3 mm and a time of 10 and 30 minutes.

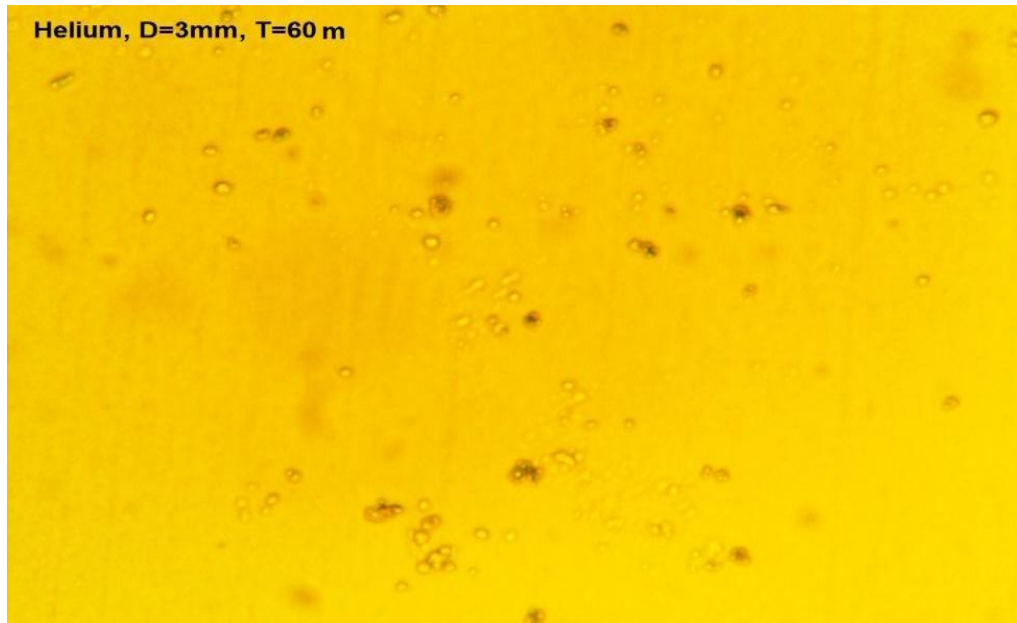
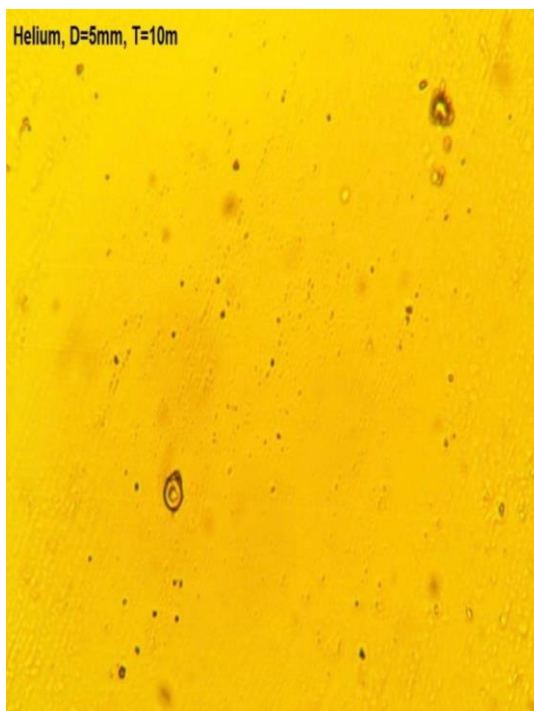


Figure 4.15. The effects of Helium plasma at a distance of 3 mm and a time 60 minutes.



(a)



(b)

Figure 4.16. The photo (a, b) shows the effects of helium plasma at a distance of 5 mm and a time 10 and 30 minutes.

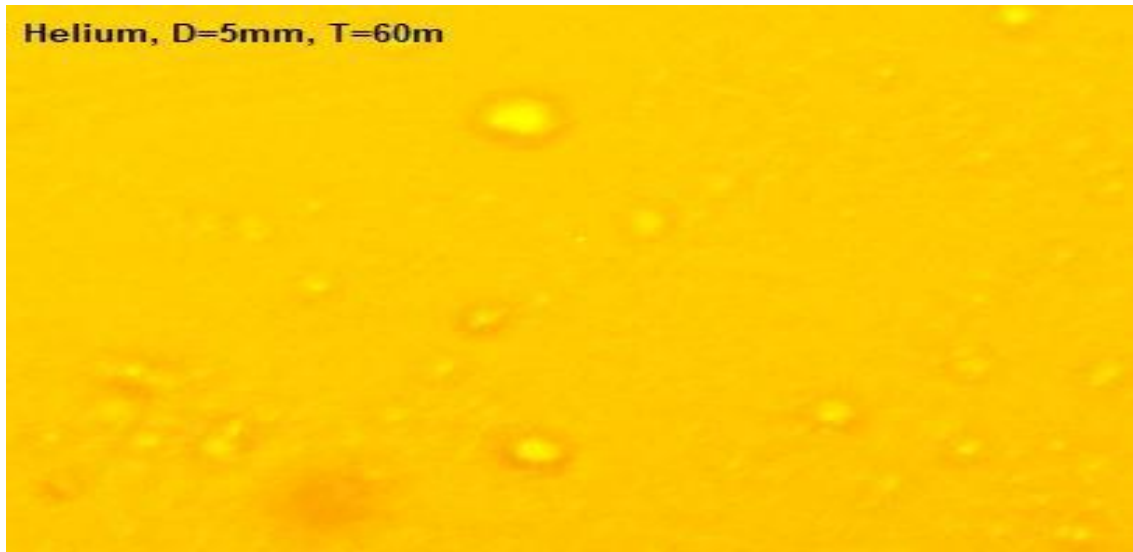


Figure 4.17. Shows the effects of helium plasma at a distance of 5 mm and a time 60 minutes.

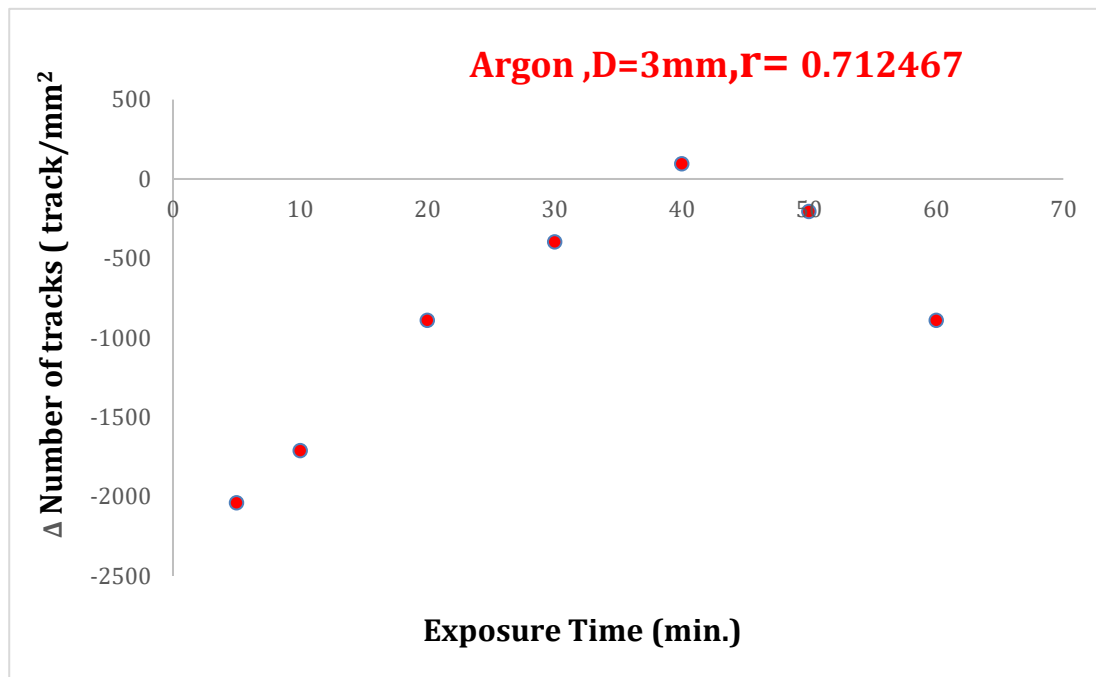


Figure 4.18. The correlation between results of chemical and plasma etching technique for Argon at D=3mm.

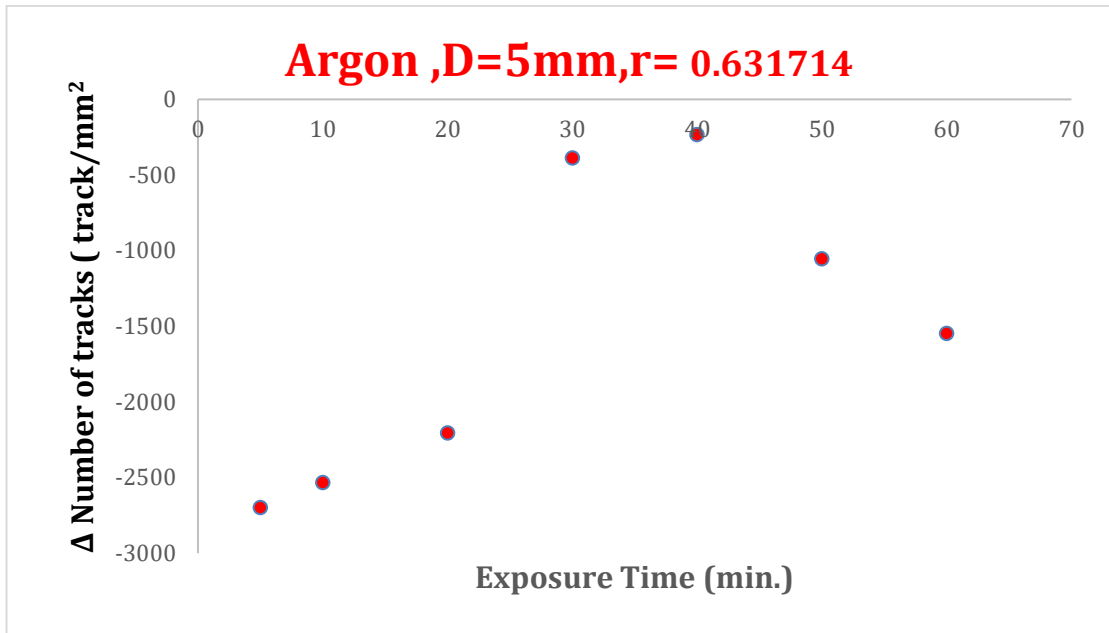


Figure 4.19. The correlation between results of chemical and plasma etching technique for Argon at D=5mm.

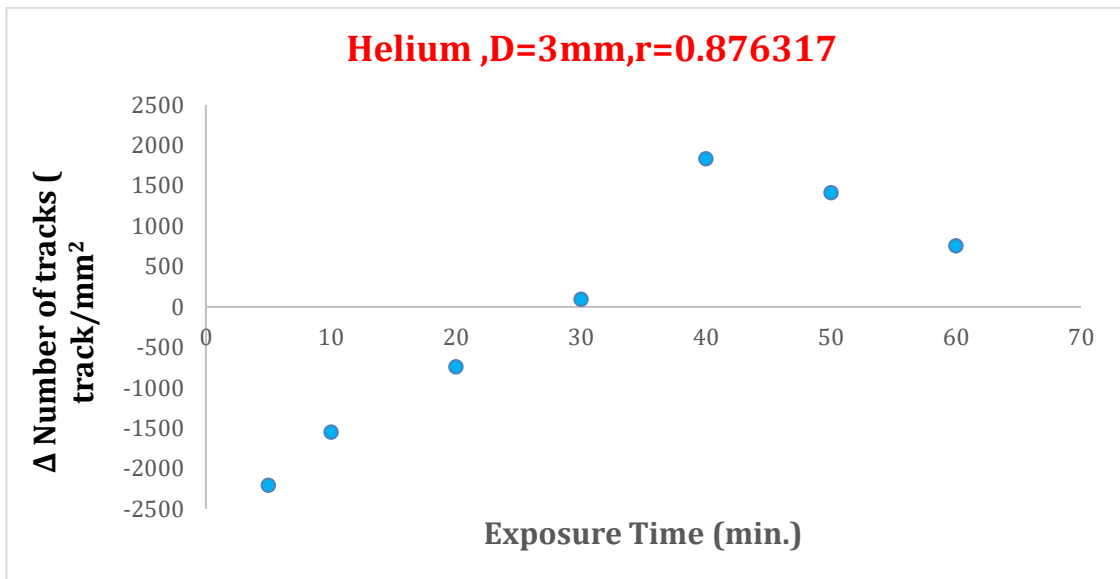


Figure 4.20. The correlation between results of chemical and plasma etching technique for Helium at D=3mm.

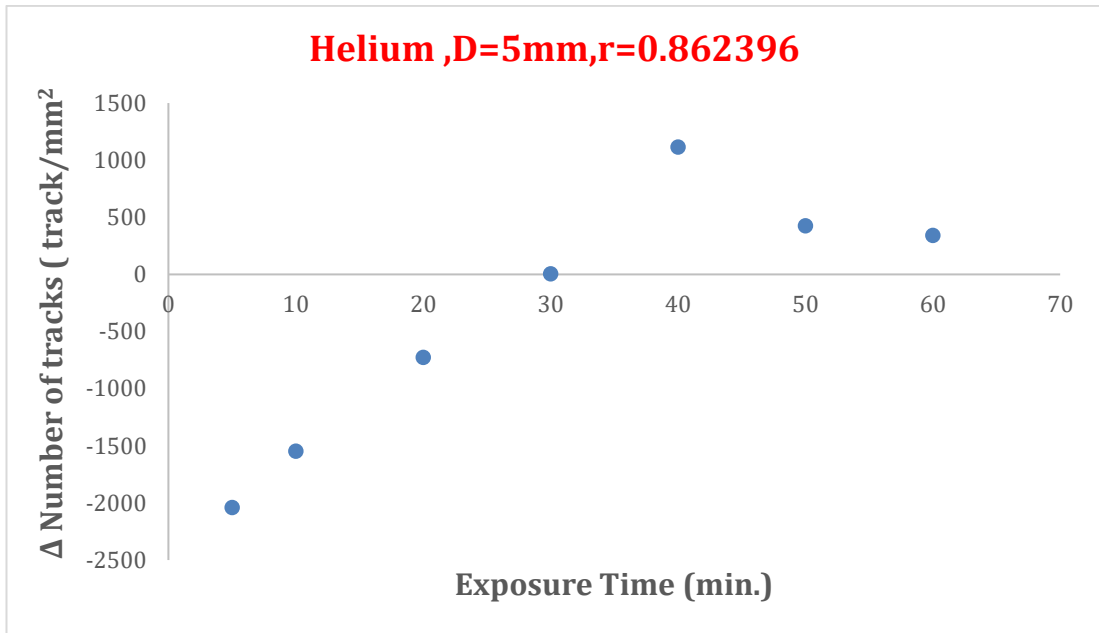


Figure 4.21. The correlation between results of chemical and plasma etching technique for Helium at D=5mm.

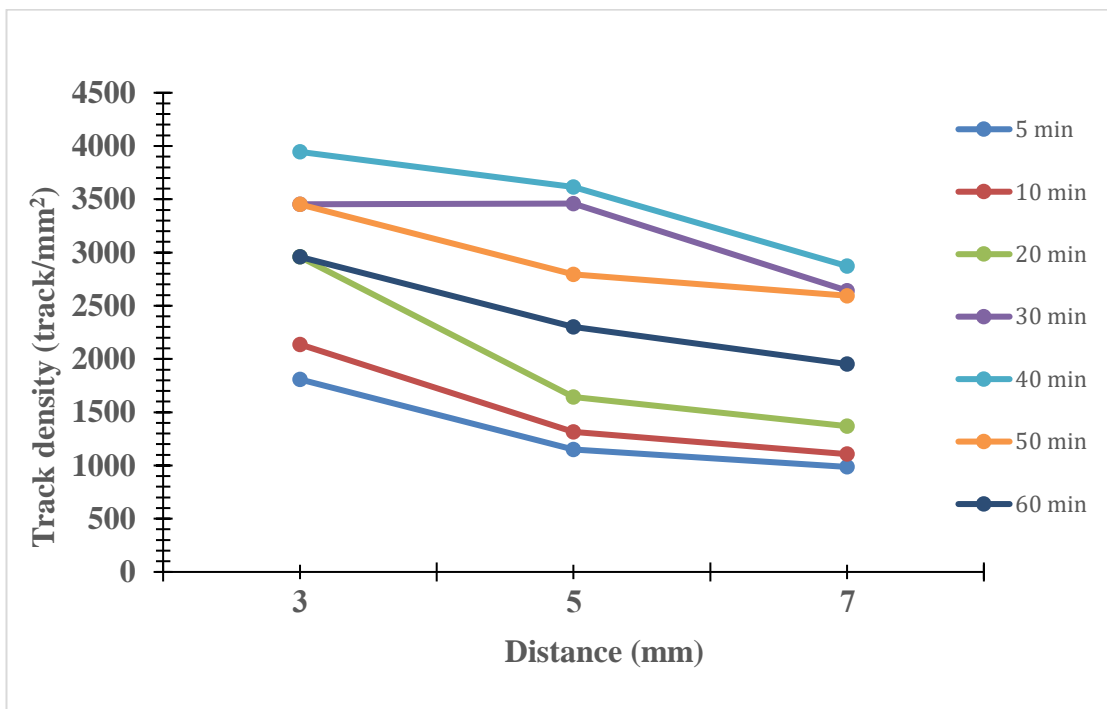


Figure 4.22. The relation between track density with distance at different times.

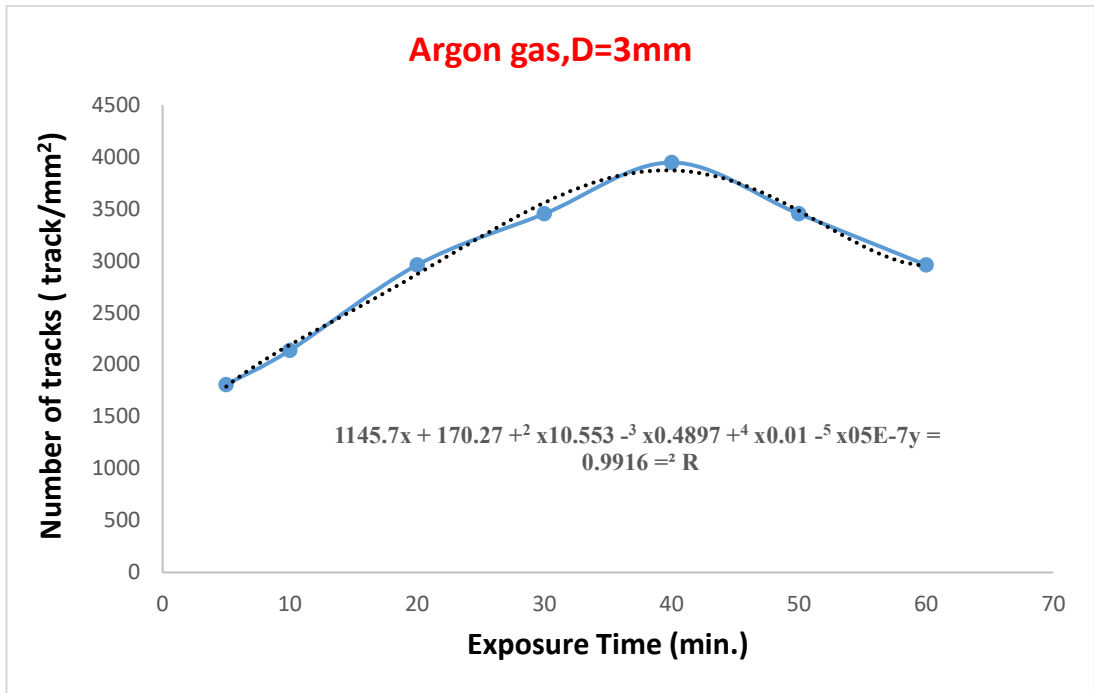


Figure 4.23. The fitting process for Argon gas at 3mm.

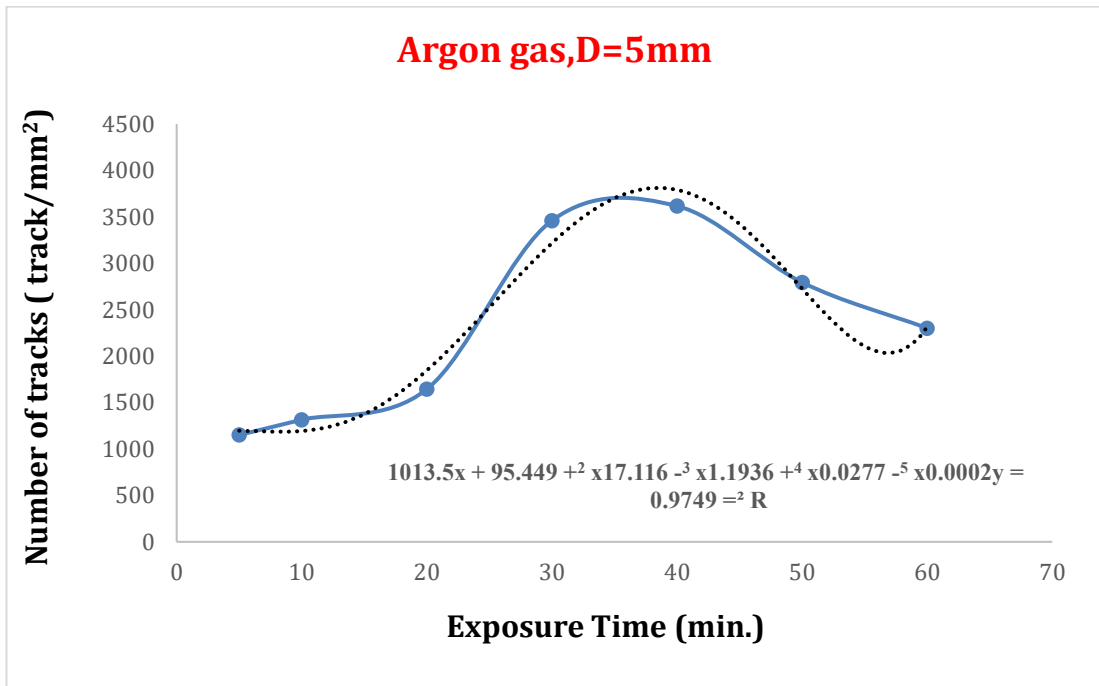


Figure 4.24. The fitting process for Argon gas at 5mm.

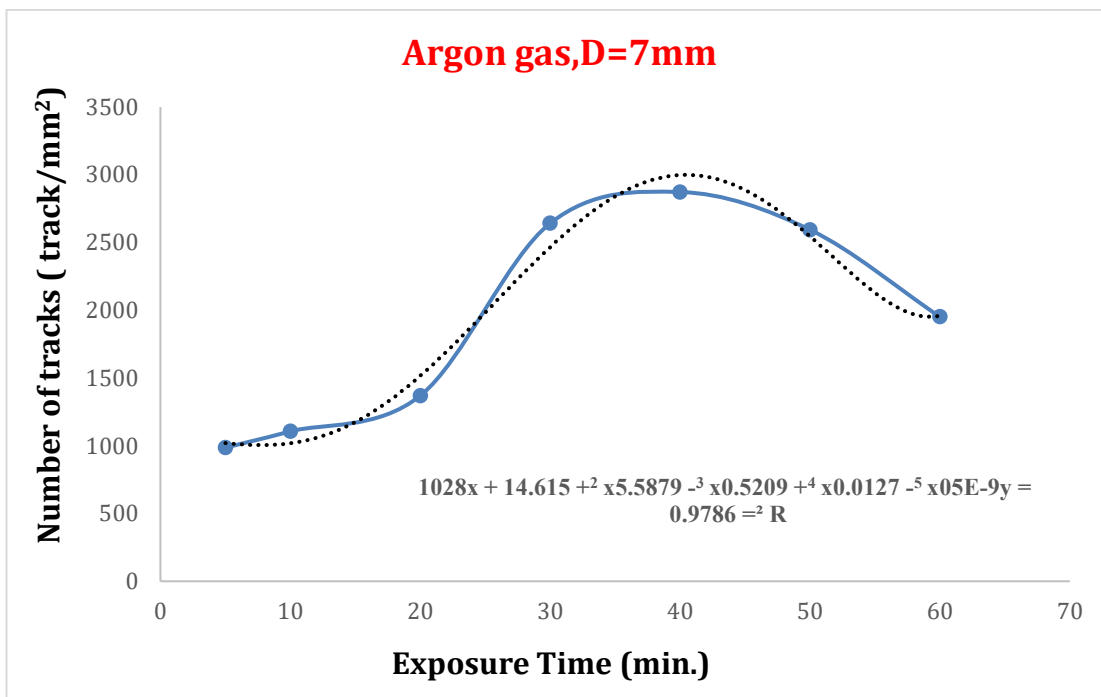


Figure 4.25. The fitting process for Argon gas at 7mm.

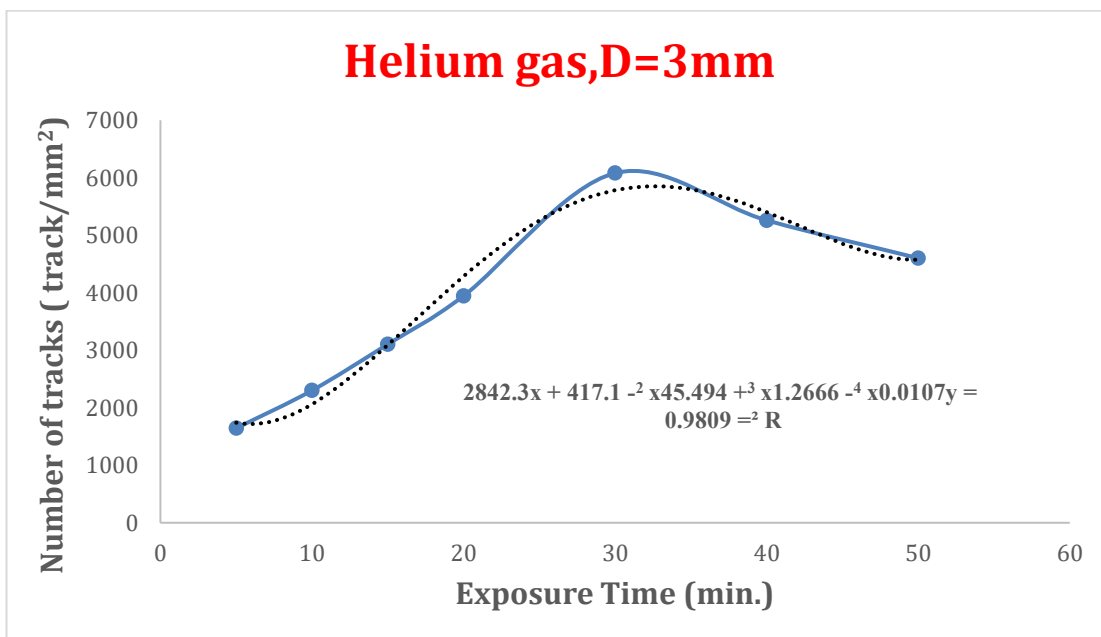


Figure 4.26. The fitting process for Helium gas at 3mm.

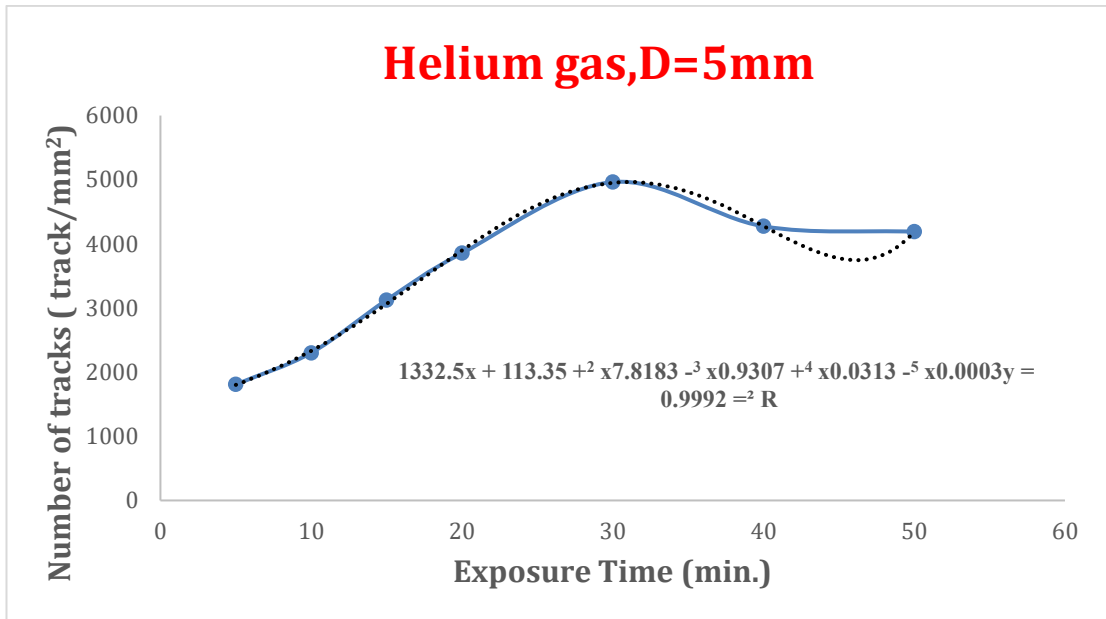


Figure 4.27. The fitting process for Helium gas at 5mm.

The values of the diameter of the track with the exposure time for each of the plasmas shown in Table No. (4.3). When drawing the relationship of the diameter of the track with the etching time. We notice that the diameter of the track increases with the exposure time to the plasma at the same distance of (3 mm) increases. Where its maximum value reaches at an exposure time of (40 minute), then the diameter of the tracks begins to decrease with Increase the exposure time for argon and helium at a fixed distance of (3mm) as shown in figures (4.28 and 4.29).

Table 4.3. The diameter of the track with the exposure time for each of the plasma.

Time (min)	Argon (3mm) D(μm)	Helium (3mm) D (μm)
0	0	0
5	10	10.2
10	13	14
20	16.7	17.2
30	18.5	18.8
40	20.2	20.9
50	18	18.3
60	16	16.5

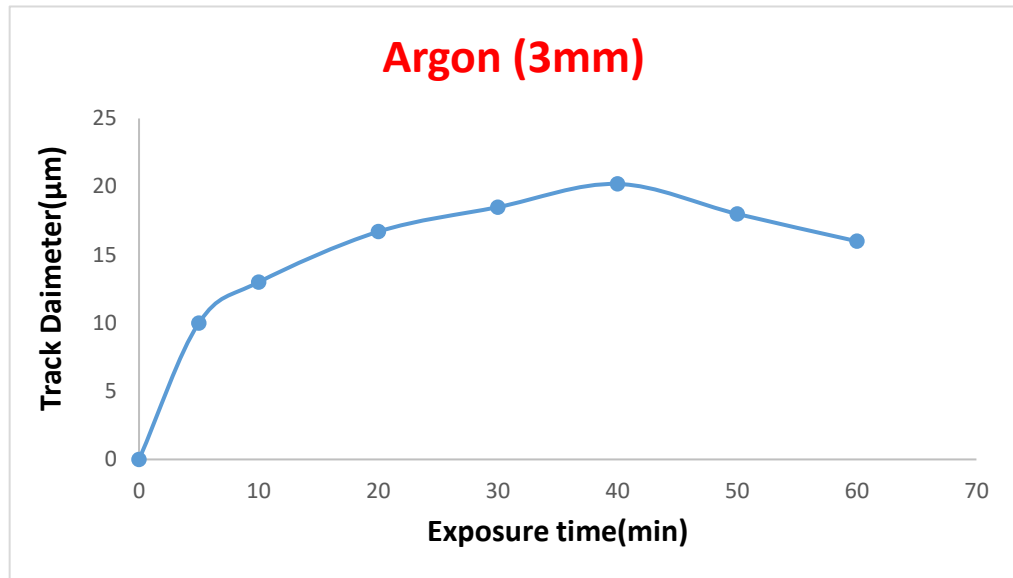


Figure 4.28. the diameter of the track with the exposure time for Argon gas at 3mm.

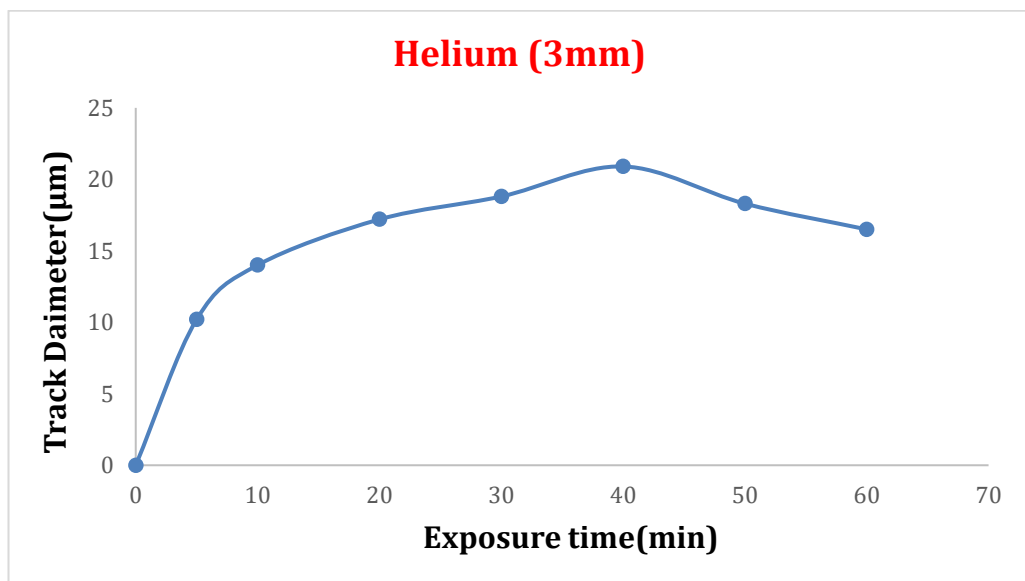


Figure 4.29. the diameter of the track with the exposure time for Helium gas at 3mm.

PART 5

CONCLUSION

From this work we can conclude the following:

- The plasma of both Argon and Helium gases can be use for etching the CR-39 detector.
- The optimal time for plasma etching using Argon gas is 40 minutes and using helium gas is approximately 40 minutes (the same).
- The correlation coefficient of the count values in the helium plasma with the count values of the chemical etching was higher and stronger than the count values in the Argon plasma.
- Accordingly, an empirical relationship can be get by fitting (which are fifth degree) to reach the complete correlation coefficient of the count values for the purpose of adopting the plasma method as an alternative method to chemical etching.
- The relationship between count values with distance is an inverse relationship and the generality of time as shown by the previous figures increases then decreases.
- The diameter of the track increases with the exposure time to the plasma at the same distance of (3 mm) increases. Where its maximum value reaches at an exposure time of (40 minute), then the diameter of the tracks begins to decrease

REFERENCES

- 1- Cassou, R. M., and Benton, E. V. (1988). Properties and application of CR-39 Polymeric nuclear track detector. *Nucl. Track Detectors*,2, pp.173-179.
- 2- Tanner R. J., Thomas D. J., Bsrlett D. T. and Harwood N. (1999). Systematic errors in the readings of track etch neutron dosimeters caused by the energy dependence of response. *Radiat.Meas.*,31, pp.483-48
- 3- Diwan, P. K., Sharma, V., Sharma, S. K., and Kumar, S.(2003) . Registration temperature effect on sensitivity of CR-39 (DOP) and SR-90 Polymer track detectors. *Radiation Measurements*, 36, 89-92.
- 4- R.A. Akber, M.A. Hary, K. jamil and H. Akhan, "Nucl. Inst and Meth.", Vol. 173, 93-96, (1980)
- 5- Fleischer, R. L., Price, P. B., & Walker, R. M. *Nuclear tracks in solids: principles and applications*. University of California Press. (1975).
- 6- Jacobson, I., Gamboa, I., Espinosa, G., & Moreno, A., Uranium determination in dental ceramics *Nuclear Tracks and Radiation Measurements*, 8(1-4), 465-467. (1984).
- 7- A. Szydowski, J. Badziak, J. Fuchs, M. Kubkowska, P. Parys, " *Radiation Measurements*", Volume 44, Issues 9–10, October–November 2009, Pages 881–884.
- 8- Naseem Salim Abdel, Munib Adel Khalil, Firas Mohammed Ali Fathi, "Determination of Optimum Etching Conditions of Nuclear Track Detector Cellulose Nitrate CN-85 for Alpha Particles", *Rafidain Journal of Science*, September 2005, 16(2):50-64.
- 9- Muhammad A. A., *Chemistry of Plastics*, Dar Al-Kutub for Printing and Publishing, University of Mosul, 1993.
- 10- Fleischer R.L., et al., " *Ann. Rev. Nucl. Sci.*", 1965. 11- Waheed, A., Manzoor, S., Cherubini, R., Moschini, G., Lembo, L., & Khan, H. A., A more suitable etching condition to register low energy proton tracks in CR-39 for neutron dosimetry, *Nuclear Instruments and Methods in Physics Research Section B: Beam Interactions with Materials and Atoms*, 47(3), 320-328. (1990).
- 12- K. N. Yu, F. M. F. Ng, J. P. Y. Ho, C. W. Y. Yip and D. Nikezic, (2004), "Measurement of Parameters Of Tracks In Cr-39 Detector From Replicas" *Radiation Protection Dosimetry*, Vol. 111, No. 1, pp. 93–96.
- 13- N. Sinenian, M. J. Rosenberg, M. J. –E. Manuel, S. C.McDuffee, Petrasso, (2012) " The response of CR-39 nuclear track detector to 1-39 MeV protons" ,

Plasma Science and Fusion Center Massachusetts Institute of Technology Cambridge MA 02139 USA.

- 14- Di, L., Zhang, J., Zhang, X., Wang, H., Li, H., Li, Y., & Bu, D. (2021). Cold plasma treatment of catalytic materials: a review. *Journal of Physics D: Applied Physics*, 54(33), 333001.
- 15- Vadikkeetil, Y., Subramaniam, Y., Murugan, R., Ananthapadmanabhan, P. V., Mostaghimi, J., Pershin, L., ... & Kobayashi, Y. (2022). Plasma assisted decomposition and reforming of greenhouse gases: A review of current status and emerging trends. *Renewable and Sustainable Energy Reviews*, 161, 112343.
- 16- VadymPrysiashnyi, *Journal of Surface Engineered Materials and Advanced Technology*, 2013, 3, 138-145.
- 17- T. Desmet, R. Morent, N. De Geyter, C. Leys, E. Schacht and P. Dubruel, *Biomacromolecules*, Vol. 10, No. 9, 2009, pp. 2351-2378. Hermsdorf, D. (2012). Influence of external and internal conditions of detector sample treatment on the particle registration sensitivity of Solid-State Nuclear Track Detectors of type CR-39. *Radiation measurements*, 47(7), 518-529.
- 18- Hermsdorf, D. (2012). Influence of external and internal conditions of detector sample treatment on the particle registration sensitivity of Solid-State Nuclear Track Detectors of type CR-39. *Radiation measurements*, 47(7), 518-529.
- 19- Hamid Hafez Mirbat Eman Kadum, Kh Nisreen, Dawser Hussain, "The use of non-thermal argon plasma as a new technique for scraping solid-state nuclear trace detectors", (Patent) University of Baghdad, March 2017.
- 20- Hassan, A. Y. (2015). Studying the radioactivity in two human organs breast and uterus using CR-39 and Lexan track detectors (Doctoral dissertation, M. Sc. Thesis, University of Al-Mustansiriyah).
- 21- Han, S. Y. (2010). Investigation of solution-based processes for functional metal oxides: printing, nanostructures, and applications.
- 22- Ostrikov, K., Neyts, E. C., & Meyyappan, M. (2013). Plasma nanoscience: from nano-solids in plasmas to nano-plasmas in solids. *Advances in Physics*, 62(2), 113-224. Tripathy, S. P. (2015). Neutron spectrometry and dosimetry using CR-39 detectors. *Solid State Phenomena*, 238, 1-15.
- 23- Fewes, A. P., & Henshaw, D. L. (1982). High resolution alpha particle spectroscopy using CR-39 plastic track detector. *Nuclear Instruments and Methods in Physics Research*, 197(2-3), 517-529.
- 24- Salih, F. N., & Jaafar, M. S. (2012). The optimum time of etching proved the Sensitivity of the CR-39 detector. *Int. J. Sci. Eng. Res*, 3(9), 1-8.
- 25- Dean, S. O. (1995). Applications of plasma and fusion research. *Journal of fusion energy*, 14(2), 251-279.

- 26- Beltrán, C. C. (2015). Fluorescent probes for selective detection of ozone in plasma applications (Doctoral dissertation, Loughborough University).
- 27- Wucher, A., Tian, H., & Winograd, N. (2014). A mixed cluster ion beam to enhance the ionization efficiency in molecular secondary ion mass spectrometry. *Rapid Communications in Mass Spectrometry*, 28(4), 396-400.
- 28- Song, S. H., & Kushner, M. J. (2012). Control of electron energy distributions and plasma characteristics of dual frequency pulsed capacitively coupled plasmas sustained in Ar and Ar/CF₄/O₂. *Plasma Sources Science and Technology*, 21(5), 055028.
- 29- C.S. Oliveira, B. Malheiros, K.C.C. Pires, M. Assunção, S. Guedes, J.N. Corrêa, and S.A. Paschuk, Low energy alpha particle tracks in CR-39 nuclear track detectors: Chemical etching studies, *Nuclear Inst. and Methods in Physics Research, A*, 995 (2021) 165130.
- 30- G.S. Sahoo, S. Paul, S.P. Tripathy, S.C. Sharma, S. Jena, S. Rout, D.S. Joshi, and T. Bandyopadhyay, Effects of neutron irradiation on optical and chemical properties of CR-39: Potential application in neutron dosimetry, *Applied Radiation and Isotopes* 94 (2014) 200–205.
- 31- L I Kravets¹, V M Elinson², R G Ibragimov³, B Mitu, and G Dinescu, Plasma surface modification of polypropylene track-etched membrane to improve its performance properties, *IOP Conf. Series: Journal of Physics: Conf. Series* 982 (2018) 012011.
- 32- Hamid H. Murbat, Nisreen Khaleel, Dawser H. Ghayb, and Fatima A. Khudair, Using non-thermal atmospheric argon plasma as a new technique in etching CR-39 nuclear track detector, Patent registered with the Central Agency for Standardization and Quality Control No. 4674 dated 8/24/2016.
- 33- Murbat, H. H., & Khudair, F. A. (2014). Generation of uniform atmospheric pressure air glow plasma by dielectric barrier discharge with glass as a dielectric. *vol. 3*, 125-131.
- 34- Yasser Yahya Qasim, & Saeed Hassan Saeed Al Nuaimi. (2018). Find the general etching rate for the LR-115 nuclear track detector. *Kirkuk University Journal for Scientific Studies*, 13(3)
- 35- https://www.researchgate.net/publication/344455694_Nontraditional_Methods_For_Different_Types_of_Solid_State_Nuclear_Track_Detectors_to_Get_Optimum_Etching_Parameters
- 36- Muhammad Al-Faytouri. (2015). The effect of ionizing and non-ionizing radiation on solid nuclear track detectors.
- 37- Tan, Y., Yuan, H., & Kearfott, K. J. (2018). Energy-dependent etching-related impacts on CR-39 alpha detection efficiency for the Rn-222 and Rn-220 decay chains. *Journal of Instrumentation*, 13(04), T04005.

- 38- Al-Jubouri, Mushtaq Abd Daoud. The effect of the concentration of the abrasive solution on the diameters of the traces of alpha particles in the CR-39 nuclear track detector.
- 39- Ahmed A.I., and Wathab H.Y., Effect of Etching Solution on Nuclear Track Detector CR-39, International Journal of Applied Engineering Research ISSN 0973-4562 Volume 13, Number 10 (2018) pp. 8659-8663
- 40- <http://www.dicoverit.com/at/phi/article.html> or Radiation Science and Health <http://ents.wpi.edu/rsh/RSH>.
- 41- Tsoufanidis N., "Measurement and Detection of Radiation". McGraw Hill Book Co., (1983).
- 42- Price P.B., Proceeding of the 10th International Conf. on SSNTDs. Bristol, (1979), p.737.
- 43- Al-Ahmad, Dr. Khaled Obaid, "Introduction to Health Physics." University of Mosul, (1993).
- 44- Singh N.P., Singh S. & Virk H.S., Nucl. Tracks, Vol.12, (1986), 793.
- 45- Durrani S.A., Proceedings of the International Symposium on Application and Technology of Ionizing Radiation, Vol.3, (1982), 1527.
- 46- Hepburn C. & Windle A.H., Journal of Material Science, Vol.15, (1980), 279.
- 47- Tommasino L. & Harrison K.G., Track Detectors of Neutron Dosimetry, No.1-4, (1985), 207
- 48- Yang C.S. & Davis C.R., Nucl. Tracks, Vol.12, (1980), 547.
- 49- Durriani S.A. & Bull R.K., "Solid State Nuclear Track Detection: Principles, Methods and Application". (1987).
- 50- Monnin M.M., Nucl. Inst. And Meth., Vol.173, (1980), 1.
- 51- Green P.F., Ramli A.G., Al Najjar S.A. & Durriani S.A., Nucl. Inst. And Meth., Vol.203, (1982), 551.
- 52- Ansari F., Nucl. Track & Rad. Meas., Vol.10, (1991), 139.
- 53- Young D.A., Nature, Vol. 182, (1958), 375.
- 54- Cartwright B.G., Shirk E.K. & price P.B., Nucl. Inst. And Meth., Vol.153, (1978), 457.
- 55- Somogyi G. & Hunyadi I., Proc. 10th Int. Conf. (SSNTDs), Lyon, 2-7 July, (1979), 443.

- 56- Raja, W. N. (2019, July). Measurement of radon concentrations in water around the northern areas of Baghdad using the CN-85 track detector. In AIP Conference Proceedings (Vol. 2123, No. 1). AIP Publishing.
- 57- Snoeckx, R., & Bogaerts, A. (2017). Plasma technology—a novel solution for CO₂ conversion?. *Chemical Society Reviews*, 46(19), 5805-5863.
- 58- Snoeckx, R., & Bogaerts, A. (2017). Plasma technology—a novel solution for CO₂ conversion?. *Chemical Society Reviews*, 46(19), 5805-5863.
- 59- V adgama, P. (2005). *Surfaces and interfaces for biomaterials*. CRC Press.
- 60- Qiu, Q. Q., Sun, W. Q., & Connor, J. (2011). *Comprehensive biomaterials. Sterilization of Biomaterials of Synthetic and Biological Origin*, 127-144.61- Berganza, C. J., & Zhang, J. H. (2013). The role of helium gas in medicine. *Medical gas research*, 3(1), 1-7.
- 62- Martusevich, A. K., Surovegina, A. V., Bocharin, I. V., Nazarov, V. V., Minenko, I. A., & Artamonov, M. Y. (2022). Cold argon atmospheric plasma for biomedicine: Biological effects, applications and possibilities. *Antioxidants*, 11(7), 1262.
- 63- Wang, R. M., Zheng, S. R., & Zheng, Y. G. (2011). *Polymer matrix composites and technology*. Elsevier.
- 64- Belkind, A., & Shapira, Y. (2011). Cold plasma etching: Fundamentals and applications. *Journal of Physics D: Applied Physics*, 44(17), 174006.

RESUME

Wisam Mahmoud ABBOUSH, He completed his primary and secondary education in the same city. He graduated from Ibn Khaldoun Preparatory School. He began his education at Tikrit University, College of Education for Pure Sciences, Department of Physics in 2016 and graduated in 2020. He began his master's studies at Karabuk University in 2022. He completed the master's program that he started in the Department of Physics in 2024 at Karabuk University, Institute of Science, Department of Physics.